UNIVERSITY OF TARTU

Faculty of Science and Technology

Institute of Physics

Kaupo Voormansik

Satellite Signal Strength Measurements with the International Space University Ground Station and the University of Tartu Ground Station

Master's Thesis

Advisors:

Prof. Joachim Köppen

D.Sc. Mart Noorma

M.Sc. Paulo Esteves

Strasbourg 2009

Dedicated to my careful mother.

Acknowledgements

I would like to thank Prof. Joachim Köppen and M.Sc. Paulo Esteves for the support during the whole work and for the critical review of the written report. Many thanks to D.Sc. Mart Noorma for the advice during initial research and help in realizing the wonderful possibility of studying in the International Space University (ISU). Thanks to Nicolas Moncussi also, who helped to repair the ISU Ground Station quickly when it was temporarily disabled in heavy rainstorm in February 2009.

I would also like to thank Estonian Information Technology Foundation, Skype and Foundation Archimedes whose financial support made the studies in the International Space University possible and thus gave a very valuable experience.

Thanks also for the following people whose contribution made the work better:
Ilmar Ansko, Manabu Kawakubo, Mitsuhito Komatsu, Urmas Kvell, Silver Lätt,
Johannes Piepenbrock, John Rivett, Prof. Rein Rõõm, Marc Schwarzbach,
Graham Shriville

Table of Contents

1 Introduction

Since the launch of OSCAR 1 (Orbiting Satellite Carrying Amateur Radio) in December 1961 amateurs have successfully built and operated numerous small satellites, mainly for radio communications. These activities led to the formation of the world-wide amateur satellite union, the AMSAT, in 1969 and have demonstrated the great educational value of small space missions, by giving a first-hand practical experience in satellite communications not only to many amateurs but also to school students. Furthermore, engineering departments of numerous universities have offered their students to design and build small spacecrafts, which gives them a valuable hands-on learning experience.

Recently, the cubesat offers a standardized approach for building space payloads at much lower costs than traditional satellite missions. The cubesat project being initiated in 1999 defines a tiny satellite with volume of 1 liter and mass less than 1 kg using amateur radio communications. Since then the specification (Lee, 2008) has evolved and numerous cubesats have been built by university students all around the world.

The ISU Ground Station, only set up in August 2008, is one of newest members of the Global Educational Network for Satellite Operations (GENSO). The GENSO is a wonderful initiative of better coordinating the amateur band Ground Stations usage by forming a network. The main principle of the GENSO is allowing remote access for the member Ground Stations. A satellite operator can use other Ground Stations in the network besides the home one to communicate with its satellite. Even more important than sharing the resources is sharing the knowledge and experience through this cooperation.

The author had a great opportunity to be one of the first serious users of the ISU Ground Station and thus explore its capabilities. The main goals of the work were to study the ISU Ground Station characteristics and use it for measuring cubesat satellite signal strengths. The measurements demonstrated that every pass is a unique mixture of satellites, Ground Stations and atmospheric propagation properties, revealing many interesting signal behavior effects.

The work consists of six Chapters. In Chapter 2 the fundamental concepts of satellite communications are given to build the necessary theoretical basis for the measurements.

Chapter 3 describes the ISU Ground Station characteristics including the transceiver calibration results and some initial manual measurements to search the ground for the fully automatic measurements introduced in Chapter 4. Chapter 4 is the main body chapter of the work discussing the automatic measurement results together with possible explanations for the signal behavior observed. Chapter 5 describes the new University of Tartu Ground Station (set up in autumn/winter 2008) with a brief sample measurement analysis. Finally in Chapter 6 the most important results are concluded and recommendations for future works are given.

2 Satellite Communication Link Basics

During its way from the transmitting satellite to the receiving Ground Station the signal encounters various losses. The situation is depicted on Figure 2.1.

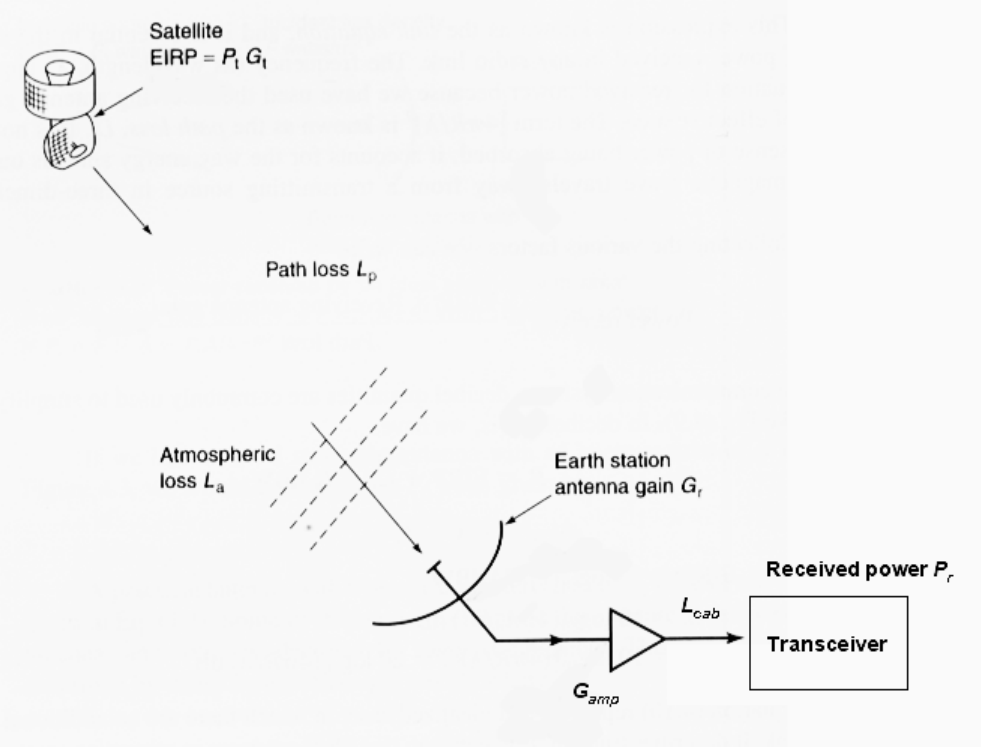

Figure 2.1 The signal propagation from the satellite to the Ground Station (Pratt, 2003).

The transmitted power (P_t) is concentrated at the main direction by the factor of gain (G_t) of the transmitting antenna. During its path big fraction is lost to space (L_p), because the emitted flux is spread over a huge area when far from the radiator. Another fraction of the signal (L_a) is lost when the signal reacts with the molecules of atmosphere. Then the received signal is amplified by the factor of gain of the receiving antenna (G_r) and by factor of gain of the low noise amplifier right after the antenna (G_{amp}), finally some part of the signal is lost in the cabling before the transceiver (L_{cab}). The received power can be described with the Friis transmission formula (Kraus, 2002) given below. To simplify the calculations decibel scale is used.

$$P_r = P_t + G_t + L_p + L_a + G_r + G_{amp} + L_{cab} \quad (2.1)$$

For LEO satellites the only parameter which remains significantly variable is the path loss (L_p, sometimes also referred as free space loss). The path loss is dependent on the distance and the wavelength of the signal, the formula in decibel scale is given below.

$$L_p = -20\log(\frac{4\pi R}{\lambda}) \qquad (2.2)$$

Besides the gain of antenna half power beam width (HPBW) is another important parameter describing the performance. The HPBW is the angle between two directions of the antenna main lobe where the power is half from the maximum, i.e. 3 dB down from the maximum value.

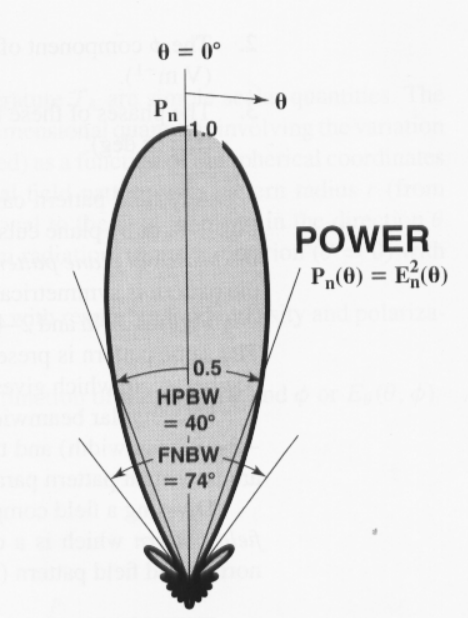

Figure 2.2 The half power beam width (HPBW) of an antenna (Kraus, 2002).

The higher is the gain of the antenna, the narrower is the HPBW. The approximate relation between the HPBW and the gain of the antenna is given with the following formula (Kraus, 2002):

$$G = \frac{40000}{\Theta_{HP} \cdot \Phi_{HP}} \cdot k \qquad (2.3)$$

Here Θ_{HP} and Φ_{HP} are the antenna HPBW-s in degrees for vertical and horizontal plane respectively. The k is the antenna efficiency factor ($0 \le k \le 1$), for well designed antennas k is close to 1.

3 Case Study: The ISU Ground Station

The ISU Ground Station is a member of the Global Educational Network for Satellite Operations (GENSO). The Ground Station has communication capabilities in VHF, UHF and S-band. The antenna subsystem with two VHF and two UHF aerials plus an S-band parabolic dish is depicted on the Figure 3.1.

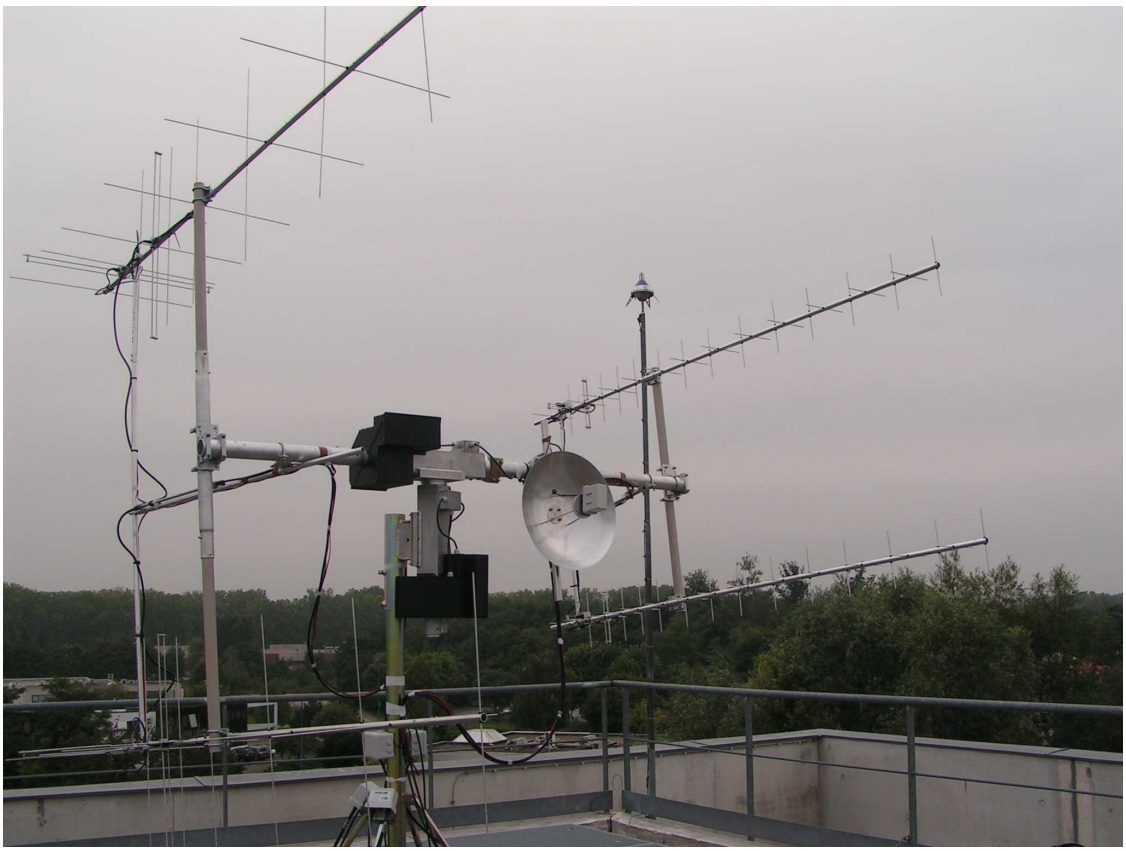

Figure 3.1 The ISU Ground Station antenna system mounted on the ISU building roof.

3.1 System Overview

The component specifications according to the manufacturer's data are given in the following table:

Table 3.1 The ISU Ground Station components specifications.

Component	**Manufacturer and model**	**Gain or loss**	**HPBW**
70 cm UHF crossed Yagi-Uda antenna	M2 Antenna Systems 436CP30	16.3 dBi (single antenna)	30º vertical and horizontal
2 m VHF crossed Yagi-Uda antenna	M2 Antenna Systems 2MCP14	12.3 dBi (single antenna)	52º vertical and horizontal
UHF pre-amplifier	SSB Electronic SP-7000	20 dB ±1 dB	-
VHF pre-amplifier	SSB Electronic SP-2000	20 dB ±1 dB	-
Transmission cable	Times Microwave LMR-600	5.6 dB /100 m (450 MHz) 3.2 dB /100 m (150 MHz)	-

The ISU Ground Station transmission/receiving system is depicted in the following block diagram. The system operates in three bands.

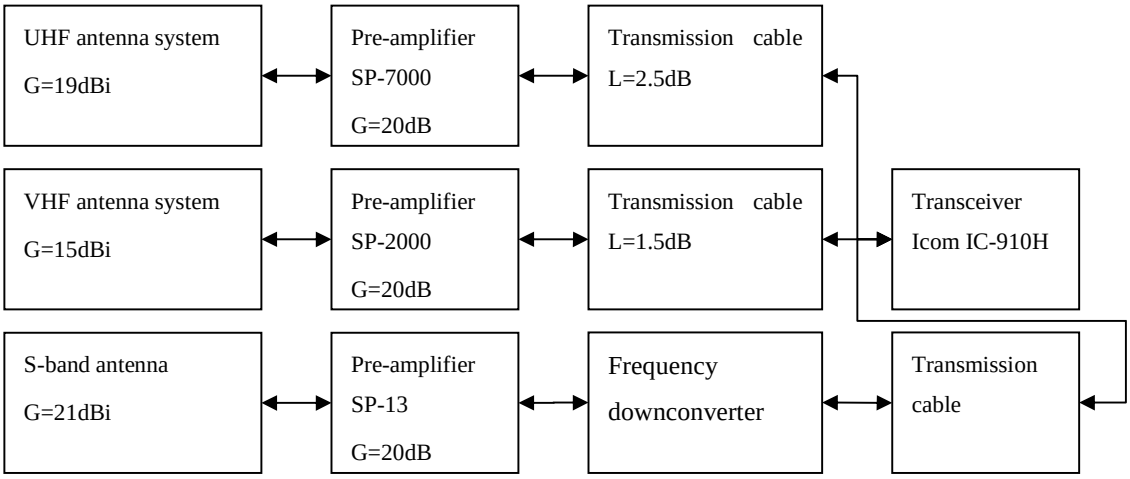

Figure 3.2 The ISU Ground Station components connection diagram.

Two vertically stacked 2x14-element 70 cm crossed Yagi-Uda antennas give a combined gain of (max.) 19.15 dBic. Stacking two identical Yagi-Uda antennas gives +3 dB gain in

ideal case, in reality the achieved gain is a little bit lower and 2.85 dB is considered as practical value (McArthur, 2002). Two vertically stacked 2x7-element 2 m crossed Yagi-Uda aerials have a combined gain of (max.) 15.15 dBic, here using again a stacking gain of 2.85 dB. The stacking distances for UHF and VHF antennas are 1.4 m and 2.4 m respectively. There is also a 60 cm diameter parabolic dish antenna with a gain of 21 dBi for the S-band.

Mast-head pre-amplifiers boost the signal right after the antennas by 20dB. This value has been measured (measurement routine is described in section 4.3). The signals are passed to the transceiver in the radio room via 45 m long coaxial cables of type LMR600. The manufacturer's data (Table 3.1) specify losses of 5.6 and 3.2 dB/100m on 450 and 140 MHz, hence the cable losses amount to 2.5 and 1.5 dB for the UHF and VHF subsystems, respectively The transceiver is an Icom IC-910H, operating on 144-146, 430-440, and 1240-1300 MHz. For the work presented here, only the 144 and 430 MHz bands were used.

3.1.1 The Antenna Pointing System

As the satellites measured were in LEO, of about 800km altitude, antenna pointing was necessary. This was carried out by M2 AZ-1000A azimuth and M2 EL-1000A elevation rotators, operated by programmable controllers RC2800PX-AL and RC2800PX-EL.

During the work with the Ground Station a systematic error of the rotator subsystem was discovered. The displayed elevation value of the rotator controller was constantly about 7 degrees higher than the real pointing elevation, as found by inspection on the roof. This gives a systematic offset of the antenna pointing and would cause about 3 dB signal loss on UHF, because the vertical HPBW (Figure 2.2) for two vertically stacked 70 cm crossed Yagi-Uda aerials is 15º.

Furthermore, an offset of +6º was also discovered in azimuth, but here the error has not so significant an effect. Since the aerials were vertically stacked the horizontal HPBW remains the same as for single antenna, hence 30º for UHF and 52º for VHF antenna array.

3.1.2 The Ground Station Software

The antenna rotators were controlled by the program Nova for Windows 2.2b (Figure 3.3), which uses the public NORAD database for the satellite orbit parameters. Transceiver frequency tuning together with the compensation of the Doppler frequency shift was carried out automatically with the Ham Radio Deluxe 4.1b software.

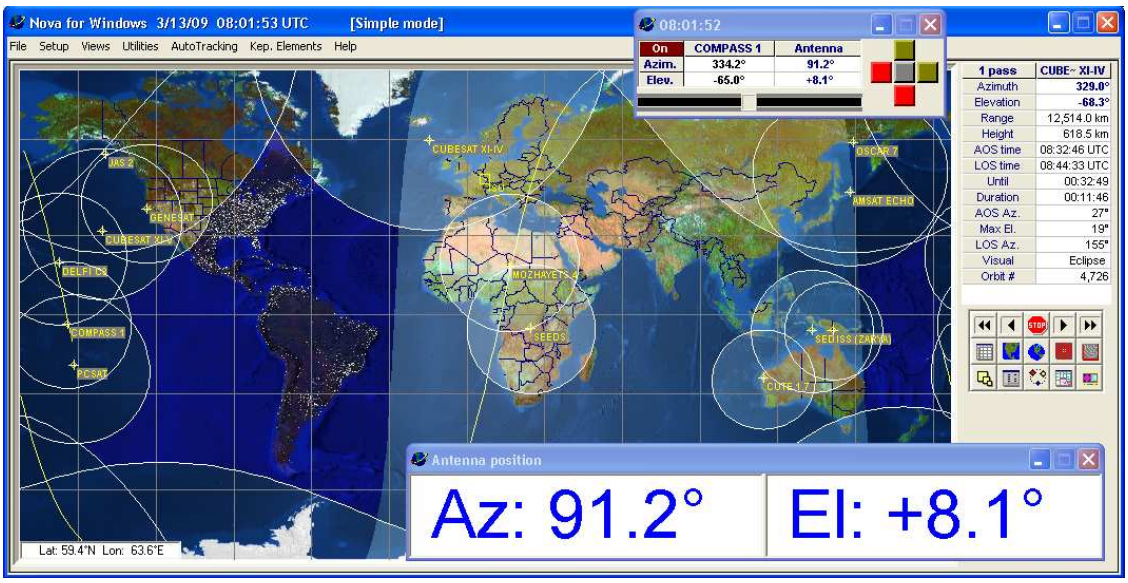

Figure 3.3 The Nova for Windows software was used for satellite tracking.

The Nova software displays the satellite visibility regions on Earth and the ground tracks. It is possible to select a certain satellite of interest and let the software to do the rotator control. During the pass relevant parameters such as the altitude of the orbit, distance to the satellite, azimuth and elevation are displayed.

The Ham Radio Deluxe (Figure 3.4) provides a user interface of the transceiver, allowing setting the frequency, switch pre-amplifier on and off, choose the modulation etc. A satellite control block is also built into the software, which allows for the automatic compensation of the Doppler shift.

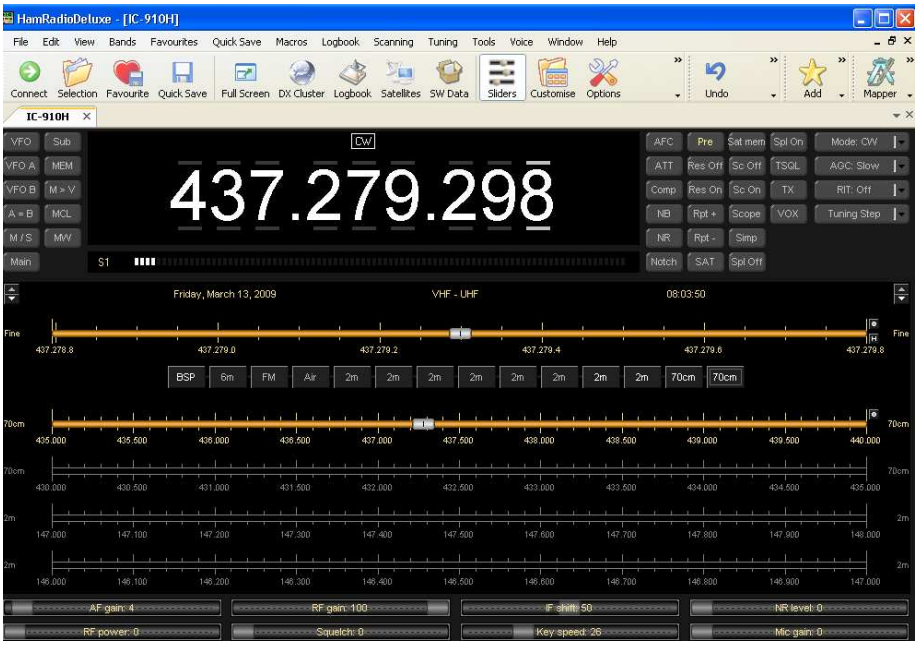

Figure 3.4 The Ham Radio Deluxe software for transceiver controlling.

3.2 How to measure satellite signal strengths

One way to measure satellite signal strengths is to use the S-meter of the transceiver. The S-values from 1 to 9 are a common measure for the signal strength used in amateur radio. The International Amateur Radio Union (IARU) recommends the S-scale as defined as follows. For frequencies above 30 MHz, S9 corresponds to a signal level of 5μV across 50 Ohms, that is -93 dBm in power; each S-step amounts to an increment of 6 dB (Table 3.2).

However, real receivers such as the Icom IC-910H, often cannot follow precisely the IARU recommendation. Therefore a calibration is needed to be able to use the S-meter readings in a quantitative way.

Table 3.2 The S-meter definition by IARU.

Ideal S-meter reading	Received voltage (μV)	Received power for 50Ω impedance cabling (dBm)
S1	0.020	-141
S2	0.040	-135
S3	0.079	-129
S4	0.16	-123
S5	0.32	-117
S6	0.63	-111
S7	1.3	-105
S8	2.5	-99
S9	5.0	-93
S9+10dB	16	-83
S9+20dB	50	-73
S9+30dB	160	-63
S9+40dB	500	-53

3.3 Calibration of the S-meter

The receiver is calibrated by applying to the antenna terminal a signal from a Marconi Instruments 2022 signal generator. Then readings from the Icom IC-910H S-meter for various input power levels were recorded.

Initially, there seemed to be a discrepancy with the signal generator's output power, which was constantly 6 dB lower than the output power calculated from the voltage that the signal generator displayed (assuming 50 Ohms impedance). The observation had actually a simple explanation. The Marconi Instruments 2022 signal generator's displayed voltage indicates the device's electromotive force (EMF) and not the potential difference (PD), as initially assumed. The EMF is exactly 2 times higher than the PD when the output is loaded with 50 Ohms, because the internal impedance of the generator is also 50 Ohms. This difference in voltage corresponds to 6 dB difference in power.

Hence to get a correct calibration one should make sure that one uses the appropriate output.

The calibration was done for both wavelength ranges: UHF on 437 MHz and VHF on 145 MHz.

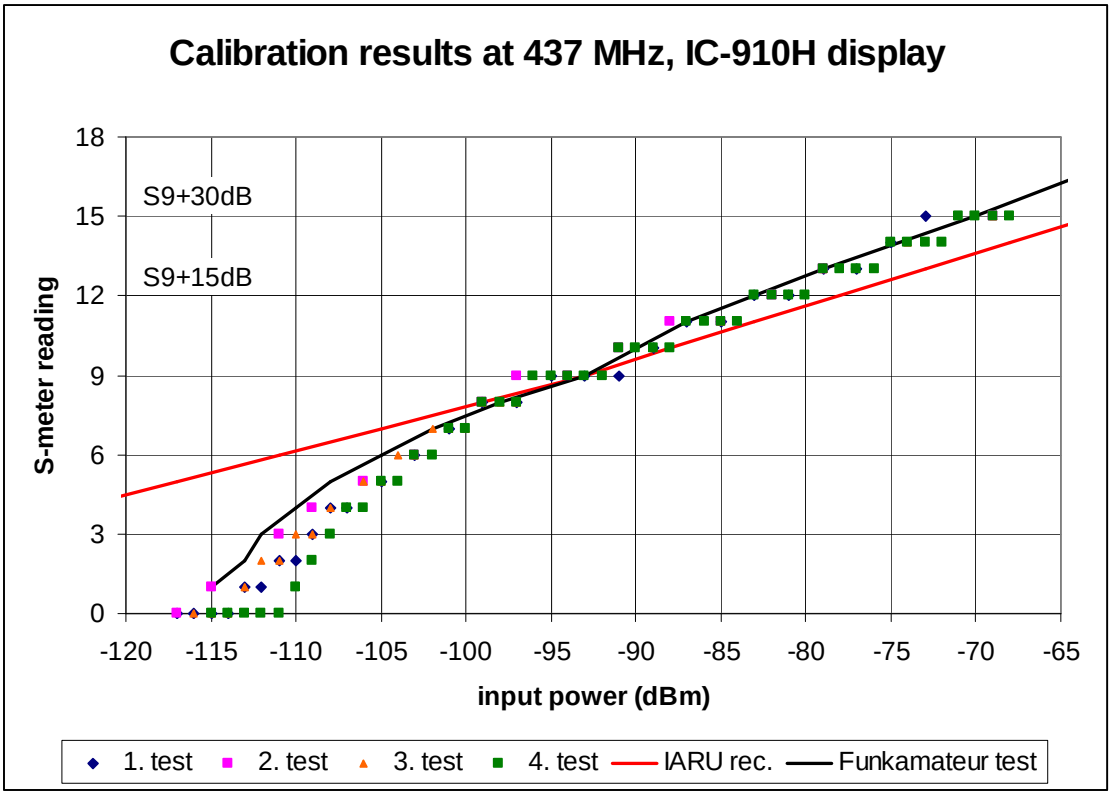

Figure 3.5 The calibration results for the IC-910H UHF input, results obtained from the transceivers display. The measurements data shown in dots is compared against the official IARU recommendation (red straight line) and the test report by Flechtner (black curve).

Figure 3.5 shows the results obtained from reading directly the Icom IC-910H display. The sensitivity above S7 follows the IARU recommended curve quite closely, with some overestimation at higher power levels. At lower power levels the transceiver's S-meter substantially underestimates the real input level. The transceiver's scale from S1 to S7 represents power levels from -115 dBm to -100 dBm, while the corresponding recommended range is from -141 dBm to -105 dBm.

The deviation around the mid-value for a given S-meter reading is from 1 dB (S5) up to 3 dB (S9).

The measurements generally confirm the behavior reported in a previous evaluation (Flechtner, 2001) as shown with the black curve. So trusting the test values without additional local calibration can be considered valid, as the difference between the published test results and the obtained mean values is only up to 3 dB.

If one tries to interpret the transceiver S-meter readings as the recommended IARU ideal values, a significant error is made, especially at low signal strengths (e.g. the transceiver's S1 reading misses the ideal value by 25 dB).

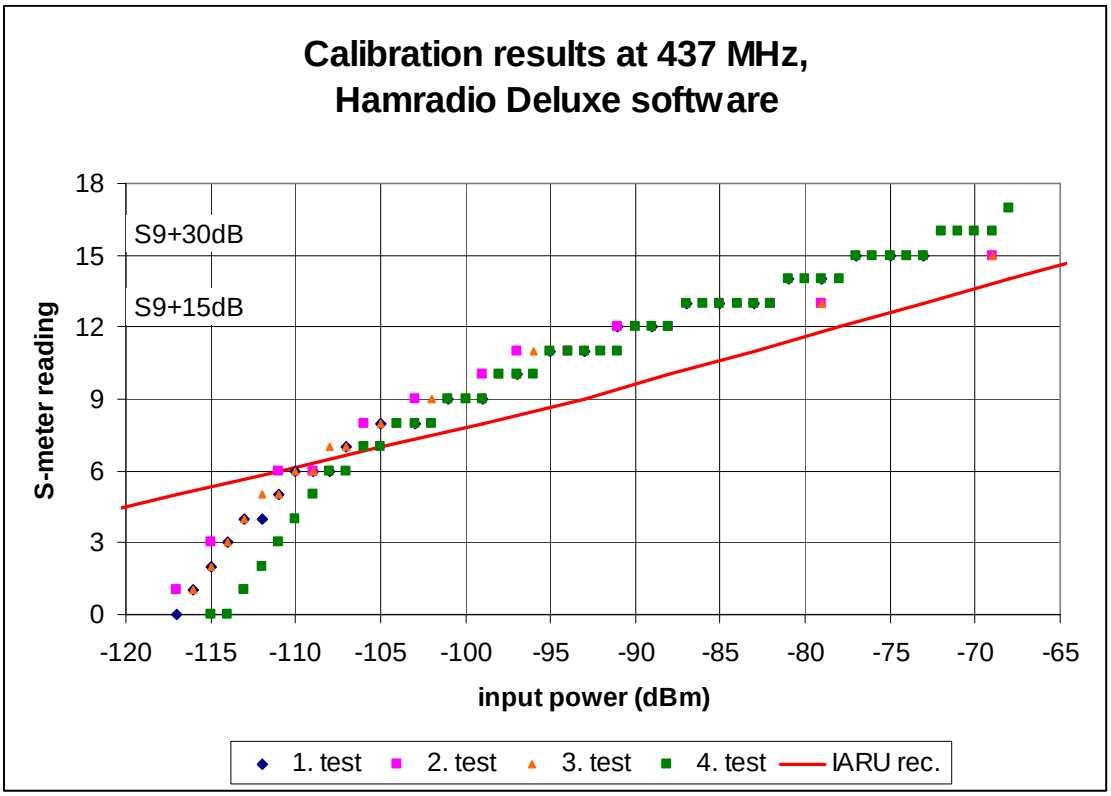

Figure 3.6 The S-meter sensitivity of UHF input according to the Ham Radio Deluxe software default settings.

The readings done with the Ham Radio Deluxe software – using the default settings - miss the IARU recommended curve even more strongly, being really close to the recommended values only around S6. Below that level the software readings underestimate the input power, showing values S1 to S6 for a range from -117 to -107 dBm, while these values should correspond to range -141 to -111 dBm, basically the same behavior as described about the Icom display readings. For signals above S6 the

measurements seem to follow a straight line with approximately the same slope as the recommended line, but overestimating it by about 6 to 9 dB.

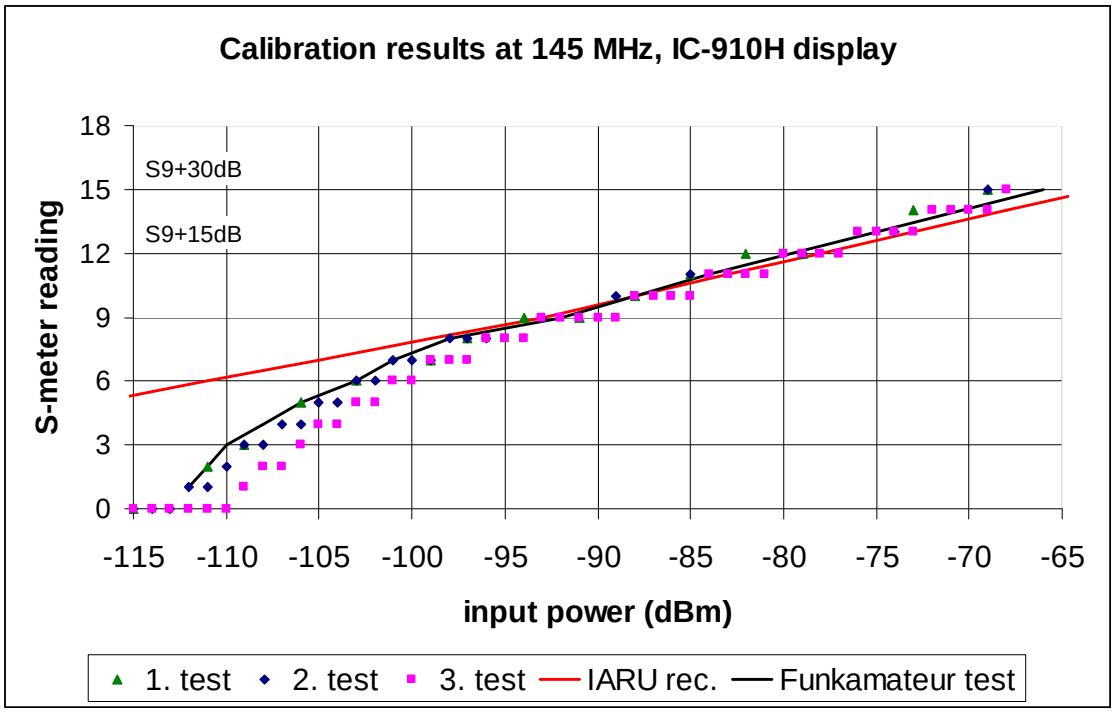

Figure 3.7 The calibration results for VHF input compared to IARU recommendation.

The calibrations for 145 MHz look very similar to the UHF results, but with slightly less scatter: The recorded S-meter mean value starting from S7 is not more than 2 dB off the published test (Flechtner, 2001).

All the data from the calibrations is given in Appendix A.

3.4 Satellite Signal Strength Measurements

A total of 20 satellite passes were observed using the ISU Ground Station. Satellites with known transmitting power were selected to be able to predict the received signal strength. This section describes the measurement procedures and represents the results.

During the whole satellite pass the S-meter of the transceiver was observed, the reading was recorded after every 200 km change in the distance. After the observations the S-meter readings were converted into power levels using the calibration results. The power at transceiver input according to the formula discussed in Chapter 2 should be:

$$P_r = P_t + G_t + L_p + L_a + G_r + G_{amp} + L_{cab} \quad (3.1)$$

All parameters are in dBs, where G_{amp} is the gain of the preamplifier and L_{cab} is the loss in the cables from antenna to the transceiver input. Taking into account that atmospheric losses vary from 0-2.1 dB for elevation angles 90º-5º respectively (Ippolito, 1986), one will not make a big error when taking atmospheric losses equal to 1 dB. When using 1 dB constantly for atmospheric losses, then the only parameter that remains variable for a certain transmitting satellite is path loss.

3.4.1 Measurements at the UHF band

The satellites observed in the UHF band were: Aachen University cubesat Compass-1 and University of Tokyo cubesats XI-IV (Figure 3.8) and X-V. The beacon output power for all of these satellites is 100 mW (+20 dBm) and the maximum gain of the dipole antenna 2 dB (Univ. of Aachen Cubesat Team, 2004 and Univ. of Tokyo Cubesat Team, 2001).

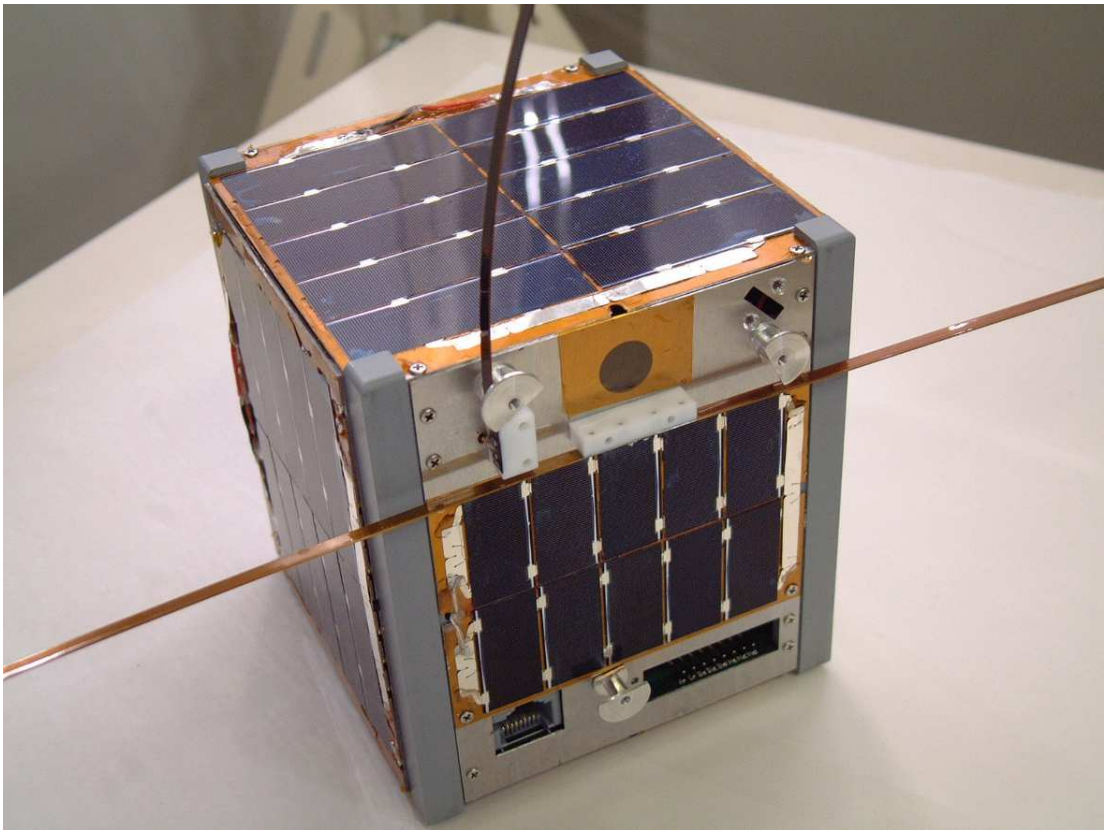

Figure 3.8 The Japanese cubesat XI-IV before the launch (Univ. of Tokyo Cubesat Team, 2003).

The received power, P_r, according to Equation (3.1) can be calculated with the actual parameters of the UHF subsystem of ISU Ground Station:

$$P_r = 20dBm + 2dB + L_p - 1dB + 19dB + 20dB - 2.5dB - 3dB = 54.5dBm + L_p \quad (3.2)$$

where $L_p = -20\log(\frac{4\pi R}{\lambda})$. For 437 MHz signal the path losses should be between -155 dB (3000 km distance, satellite close to horizon) and -143 dB (800 km distance, satellite close to zenith). The atmospheric losses were estimated to -1 dB as described at Equation (3.1). Here additional 3 dB were subtracted, because of the receiving antenna pointing error losses. The antenna elevation rotator had a systematic offset of 7º (see section 3.1.1), that resulted in approximately 3 dB loss, taking account that two vertically stacked 70cm Yagi-Uda aerials had a vertical HPBW of 15º.

The results of Compass-1 pass measured on 14.02.2009 between 12:23-12:34 are shown on Figure 3.9.

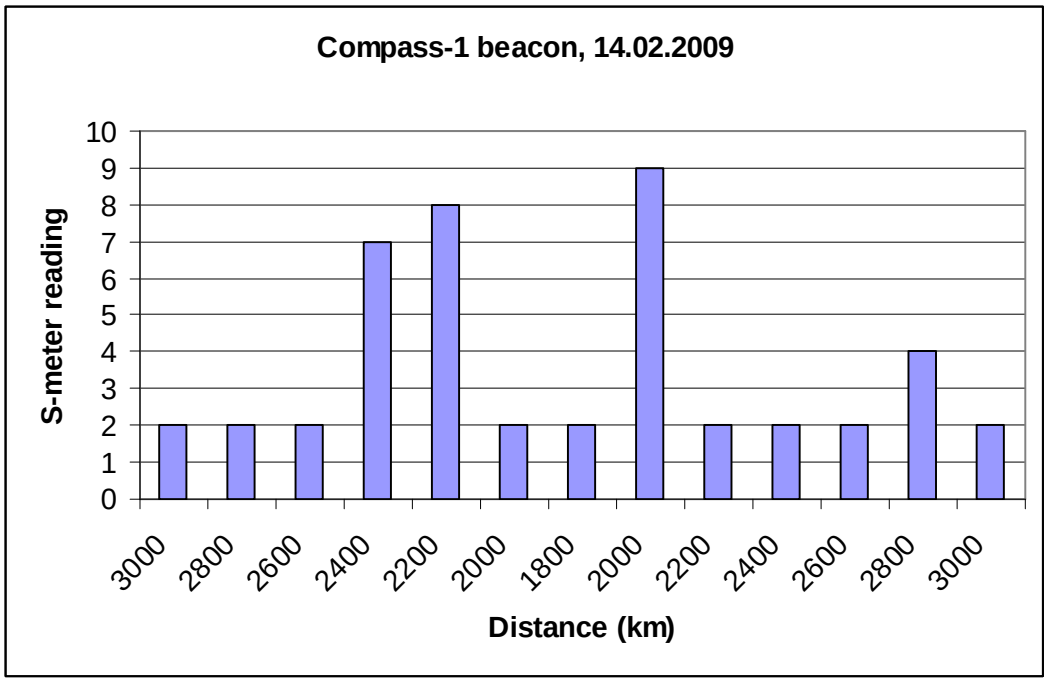

Figure 3.9 The S-meter readings for Compass-1 pass on 14.02.2009 at 12:23-12:34.

The S-meter reading stayed at S2 for the most of the time and only went up for a short time. This has a simple explanation: The Compass-1 beacon does not work in continuous mode. Instead, it transmits Morse code in short bursts with 3 minute intervals. The S-

meter reading ‘2’ during the pauses is the typical value of the noise of the UHF receiving system with pre-amplifier switched on.

The results of the Japanese cubesat XI-V pass, recorded on 15.02.2009 between 10:36-10:50, are represented in the chart below:

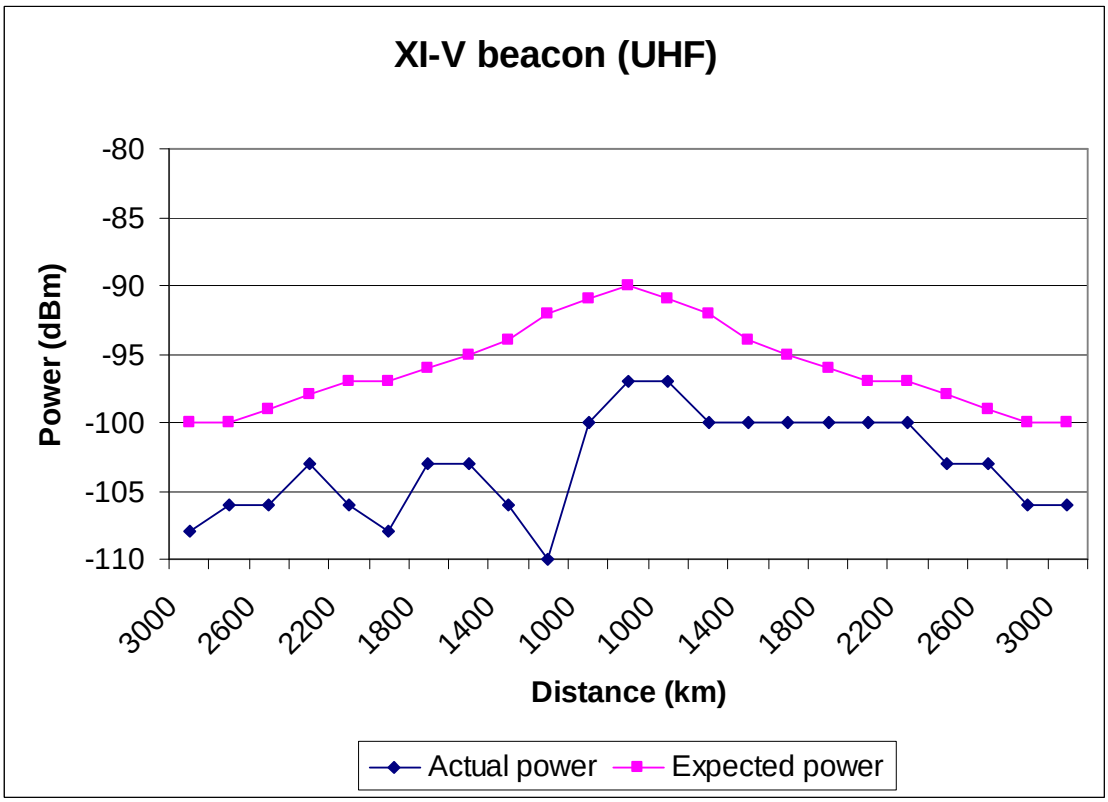

Figure 3.10 The signal strengths of XI-V cubesat beacon.

The XI-V beacon transmits Morse code continuously and here no interruptions occurred. The actual signal level generally follows the expected pattern, but is systematically lower with a few greater fluctuations.

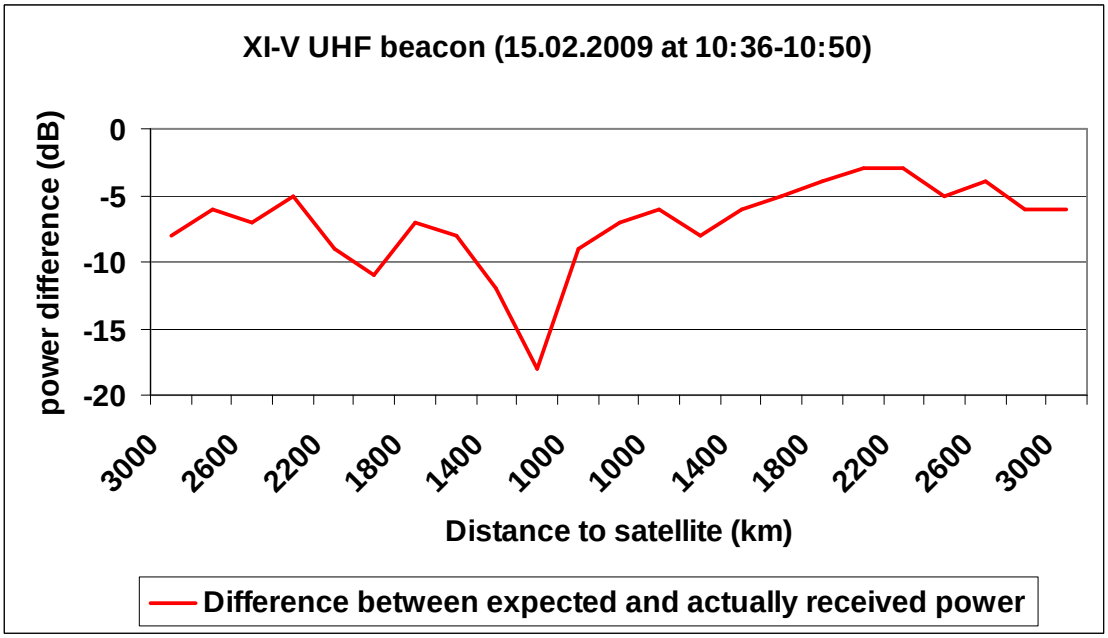

Figure 3.11 The difference between recorded and expected signal strengths.

The difference between the expected and the actual signal strength (Figure 3.11) was from -3 to -8 dB for most of the time. The error grows sometimes bigger (down to -18 dB) and is especially significant at high elevation angles when the satellite approaches the Ground Station.

In Figures 3.12 and 3.13, all recorded signal powers are plotted against range and compared with the expected power. Most of the measurements show actually weaker signals than expected, this might have two reasons:

- The actual beacon output power is less than 100 mW given in the documentation.
- There are some additional losses that had not been taken account in the received power calculations.

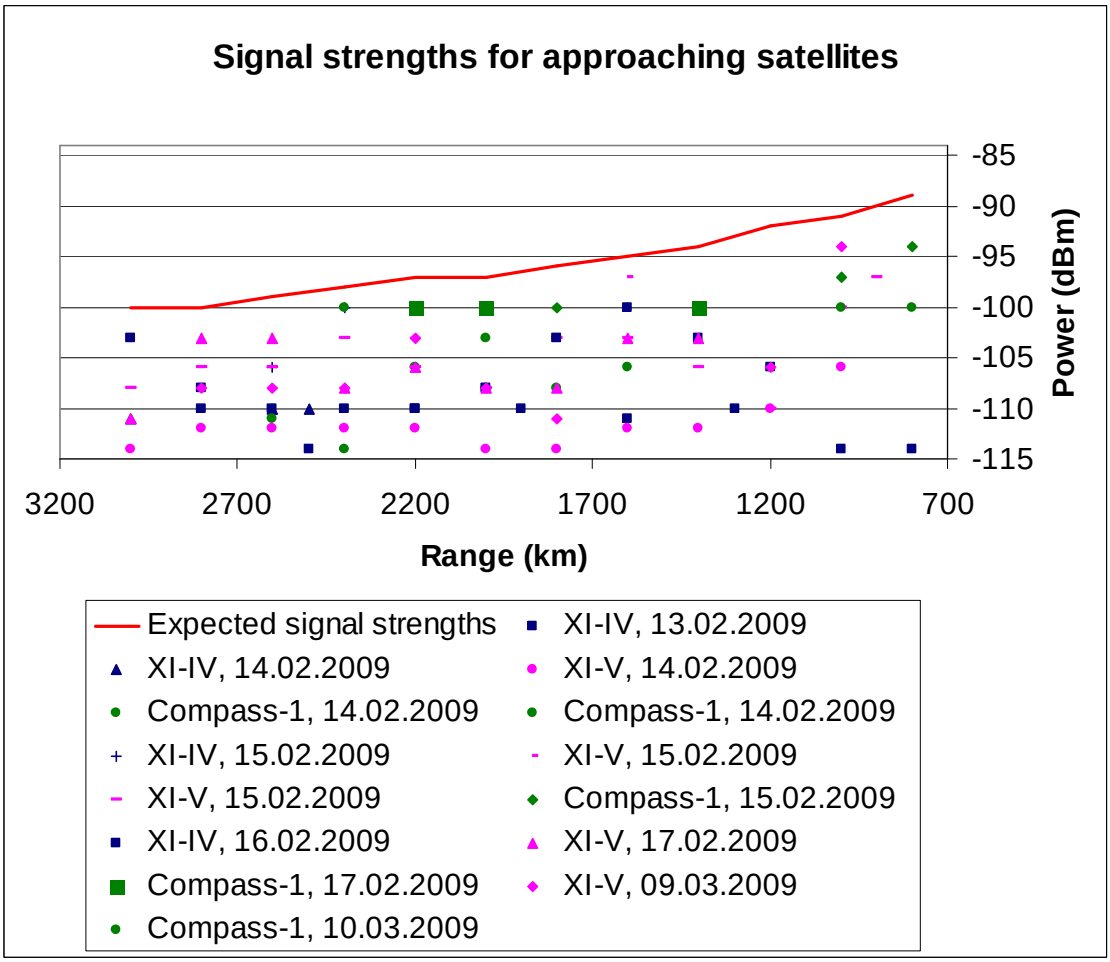

Figure 3.12 The approaching satellite signal strengths plotted against expected power curve.

In addition to being lower, the signal strengths do not appear to follow the dependence on distance as one would expect from the path loss formula. The real curves are much flatter. Furthermore, something strange seems to happen at distances 1400-1200 km for approaching satellites. The measured power levels are even lower than for longer distances.

For receding satellites the distance dependence of signal strengths is somewhat clearer, but here again the real measured values are most of the time lower than the calculated ones.

For both charts there are more measurement points for longer distances, because short distances as 800-1200 km require the satellite passing close to zenith, which does not happen very often.

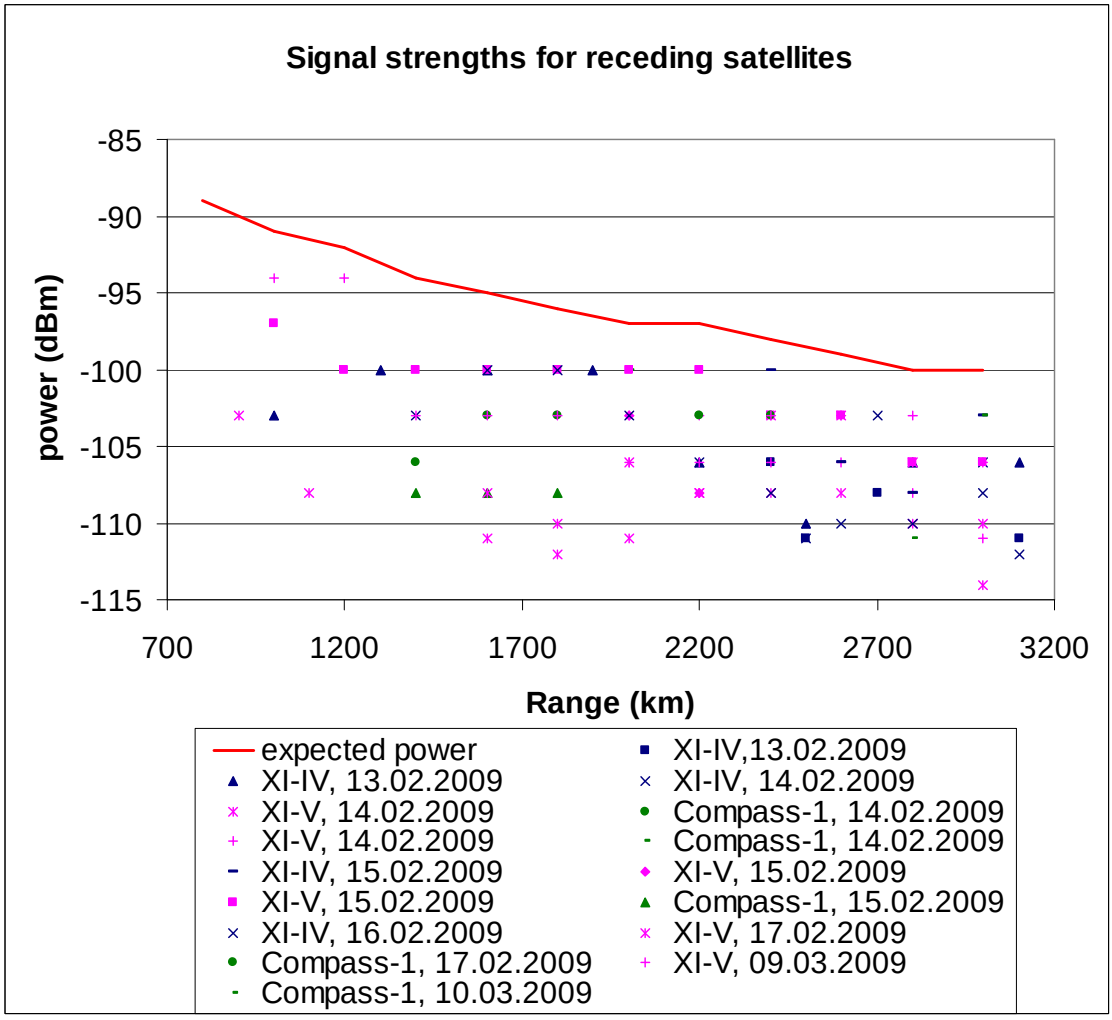

Figure 3.13 The signal strengths from the receding satellites plotted against expected levels .

3.4.2 Measurements at the VHF band

Receiving the VHF signals turned out to be more difficult. At first there are much fewer amateur radio satellites that transmit in this region, which is more often used for uplink than downlink. The choice of VHF transmitting satellites was narrowed down to three candidates: Navy-OSCAR 44, Delfi OSCAR-64 (a 3-unit cubesat) and HAMSAT, but from none of these satellites it was possible to receive signals.

The expected signal strengths of the Delfi OSCAR-64 and the HAMSAT, whose output powers were known, are given in the Table 3.3. Here again the link equation formula described in Chapter 2 was applied. Thus, it should have been well possible to pick up these signals.

Table 3.3 Expected received signal strengths with corresponding S-meter readings.

Satellite	**Output power**	**Expected received power (3000 km)**	**Expected received power (2000 km)**
Delfi Oscar-64 (TU Delft, 2008)	Beacon: 40 mW	-95 dBm (S9)	-92 dBm (S9+5dB)
	Telemetry: 400 mW	-85 dBm (S9+15 dB)	-82 dBm (S9+20dB)
HAMSAT (Amsat India, 2005)	Beacon: unknown		
	Relay link: 1 W	-81 dBm (S9+20dB)	-78 dBm (S9+20dB

Instead, a substantial level of noise was noticed on this frequency band. The noise is a rushing noise, and is present at all frequencies with about the same intensity. In order to localize and possibly identify the noise a rough map was created. The frequency for the test was chosen 145.900 MHz, the middle of the 2m band's section (145.800-146.000 MHz) allocated for the amateur satellite services. During the test pre-amplifier was switched on. The antenna pointing at vertical was with maximum 25º steps and 30º in horizontal. The pointing resolution should be precise enough, because the two vertically stacked VHF antennas together have a HPBW of 26º in vertical and 52º in horizontal. The test was done twice on different days. The results are shown in the following charts, complete test logs are given in appendixes.

It can be seen from the charts that generally there is much more noise close to the horizon than for higher elevation angles and the noise is also strongly azimuth dependent, being especially strong at East (azimuths from 90º to 120º) and West (azimuths from 270º to 300º) .

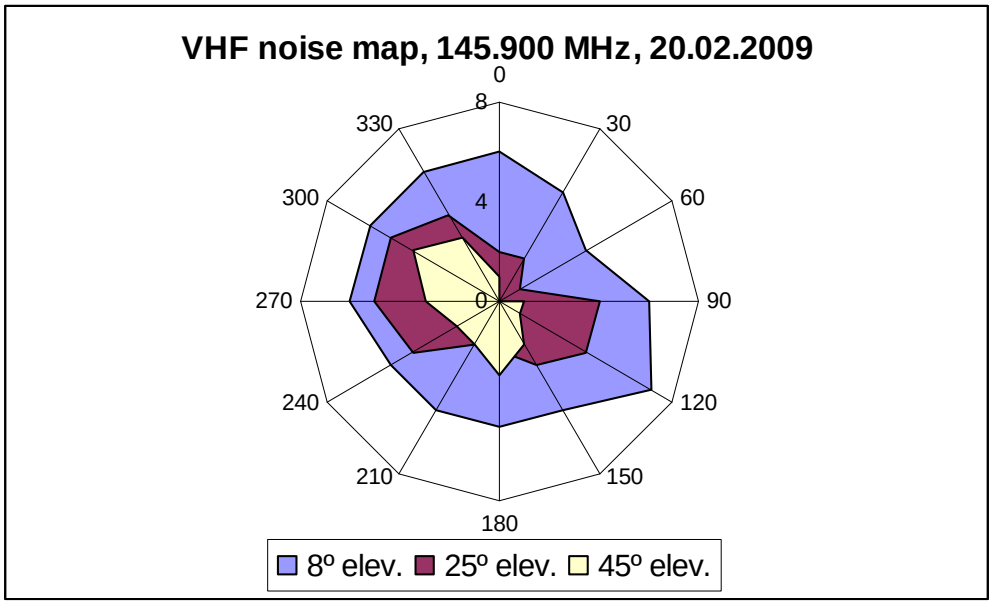

Figure 3.14 VHF noise map of ISU Ground Station, test done at 17.00 in the evening.

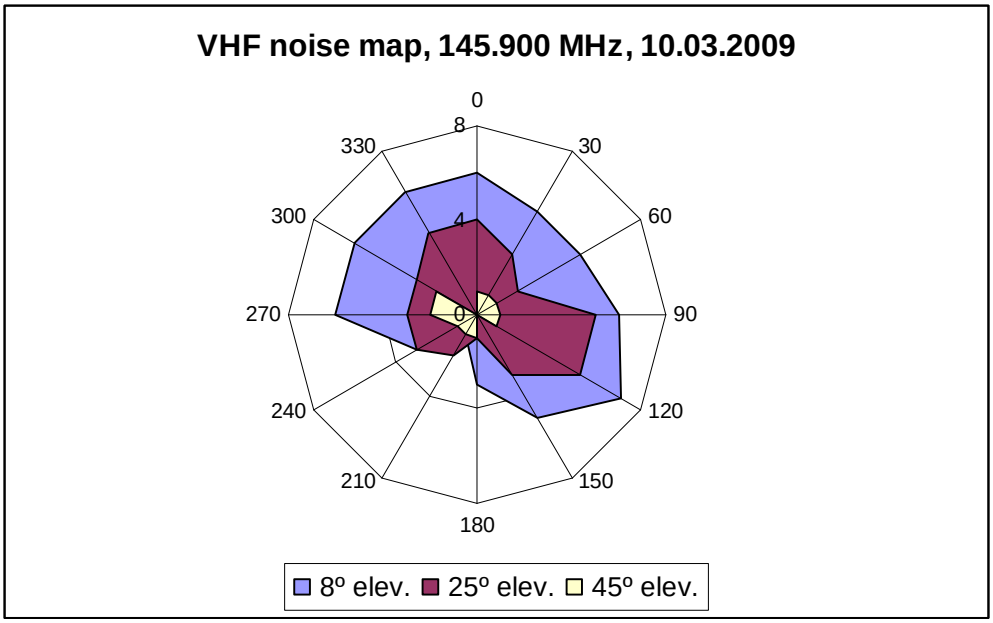

Figure 3.15 VHF noise map of ISU Ground Station, test done at 14.00 afternoon.

When looking at the ISU Ground Station's surroundings in a map (Figure 3.16), it is easy to see that at South and South-West directions there are no buildings close to ISU within a 400 m radius. On the other hand there are several buildings close to ISU towards West/North-West and East. At azimuth 120º where the noise peak occurs (according to both measurements) lay some hostelry and sport facilities.

Figure 3.16 Aerial view of the ISU neighborhood, superposed with the data of the noise survey from Figure 3.15. The added boxes show new buildings which were not present when the image was taken (Google Earth, 2009).

It is easy to see that from South to West where no buildings lay close to ISU Ground Station there is little noise, even with the first measurement. With the second measurement (as depicted on the figure above) the picture is even clearer. At noise peak direction (azimuth 120º) there are some new buildings close to the Ground Station. The light blue box is a 3-floor fitness studio and the striped box is a 6-floor extension to the hotel near it. The exact source of the noise is unclear yet, but it is very likely that it is coming from these new buildings.

Now comparing the recorded noise levels with the expected signal strengths of Table 3.3, it is clear that satellite signals should still be stronger than the terrestrial noise. For the worst case of listening to the Delfi Oscar-64 beacon close to horizon at azimuth 120º the expected signal strength of S9 should be still 2 S-units stronger than the noise (S7) there. Hence there should be additional reasons for not detecting the VHF satellites. To clarify that issue repeated measurements should be carried out.

3.4.3 Problems Faced

The main problems faced were connected with the antenna pointing system. The rotator cannot turn more than 356 degrees. Every time the satellite moved over the 0 degrees azimuth limit the rotator had to execute one full turn that takes about 2 minutes out of the valuable connection time.

The tracking software Nova for Windows together with the hardware interface turned out to be also a bit unreliable. During the initial pointing towards the satellite the system hung up several times and needed re-start. This problem could actually be easily mitigated with preparing all the satellite passes well in advance (at least 15 minutes before the session beginning), to be able to discover the problem before recording starts and re-start the tracking system if necessary.

The situation was worse when the problem occurred during the recording as it happened with the XI-V signal recording on 09.03.2009 (see Appendix B for the original data). The initial pointing did go well and the azimuth tracking was operating also, but the elevation controller hung up. The problem was discovered when the elevation to the satellite was 15º (2000 km) and the tracking system was finally recovered at elevation 35º (1200 km), after switching the antenna rotator controllers physically off and then on again. This and other similar events when the rotator system had trouble with tracking the satellite are indicated in the recording logs with ‘rotator problems’ (see Appendix B for details).

3.5 Performance Evaluation

The received signal levels were generally lower than the expected values. The difference between predictions and reality were about 7 dB for most of the time. One cause could be the degradation of the power system of spacecraft, instead of 100 mW, the actual output power can be lower. Cubesats are designed for relatively short lifetime (active mission time up to 2 years usually), the launch dates plotted against average signal strengths are depicted on the Figure 3.17

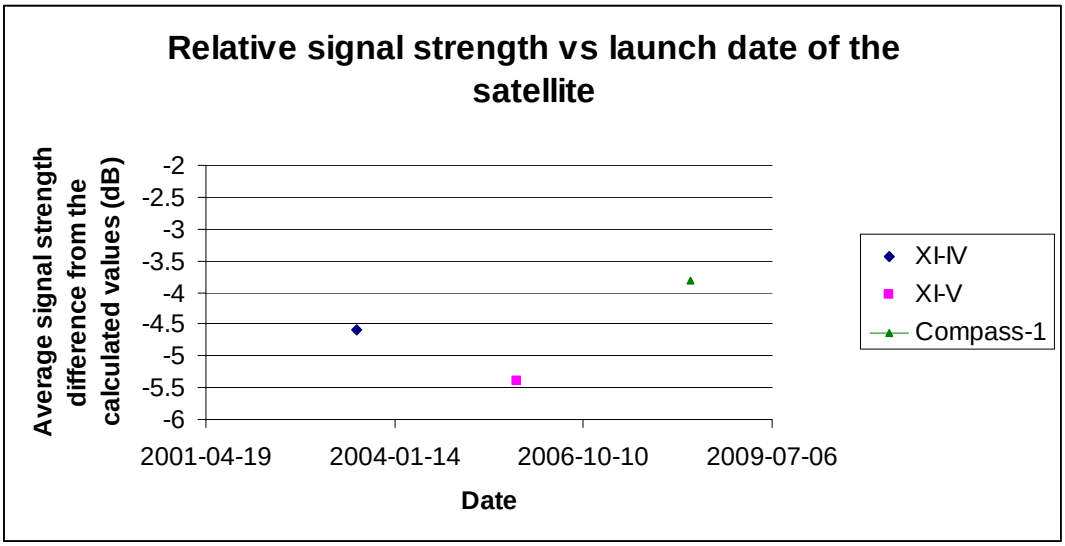

Figure 3.17 The average signal strength difference from the expected value of three strongest passes for each of the observed Cubesats.

As seen from Figure 3.17 the youngest satellite (Compass-1) indeed gives a signal closest to the expected values. But contrary to expectation, the older XI-IV seems to be in better condition than the two years younger XI-V.

Sometimes the gap between expected and actually received powers was as large as 17 dB, especially for shorter distances and approaching satellites. It was initially assumed that there could be something wrong with the Doppler Shift corrections that were carried out automatically with the Ham Radio Deluxe software. This is actually not very likely reason, because no significant change in the Morse code tone was observed and the tone is highly dependent on the Doppler Shift errors.

4 Measurements with the ISU Ground Station Using Automatic S-meter Capturing

For getting a better understanding of all the questions raised in the previous preliminary measurements more and higher quality data was needed. To permit an automatic recording of the S-meter data the software IC910Tester was written by Prof. Joachim Köppen.

4.1 Software Overview

The main purpose of this JAVA software was to provide a fully automatic recording of the signal strengths, by requesting via a serial port the Icom IC-910H transceiver to send its 'S'-meter readings. The signal strengths are written to a text file and are also displayed live in a chart (see figure below). The actual sampling rate was about 1 second.

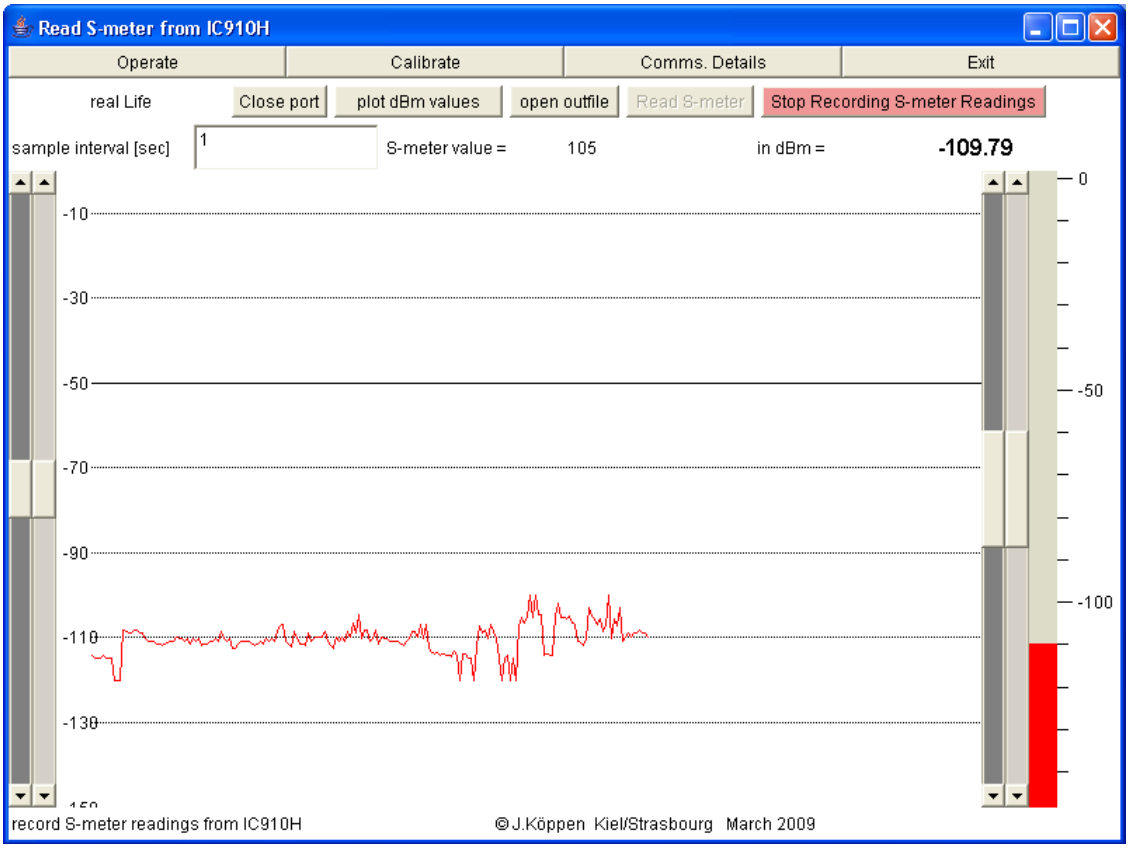

Figure 4.1 The IC910Tester software, recording the S-meter values and displaying the results chart simultaneously.

4.2 Calibration of the Software S-meter Readings

As the signal strength output to the serial port is given in the form of some integer numbers, a calibration was needed. The calibration functionality was built in to the software and the routine was relatively easy. Here again the Marconi Instruments 2022 Signal Generator was used. The input signal was varied in 1 dB steps and for each of the signal levels the output integer value from the software was recorded.

The calibration results for 144 and 430 MHz are shown in the figure below, detailed results are given in Appendix D.

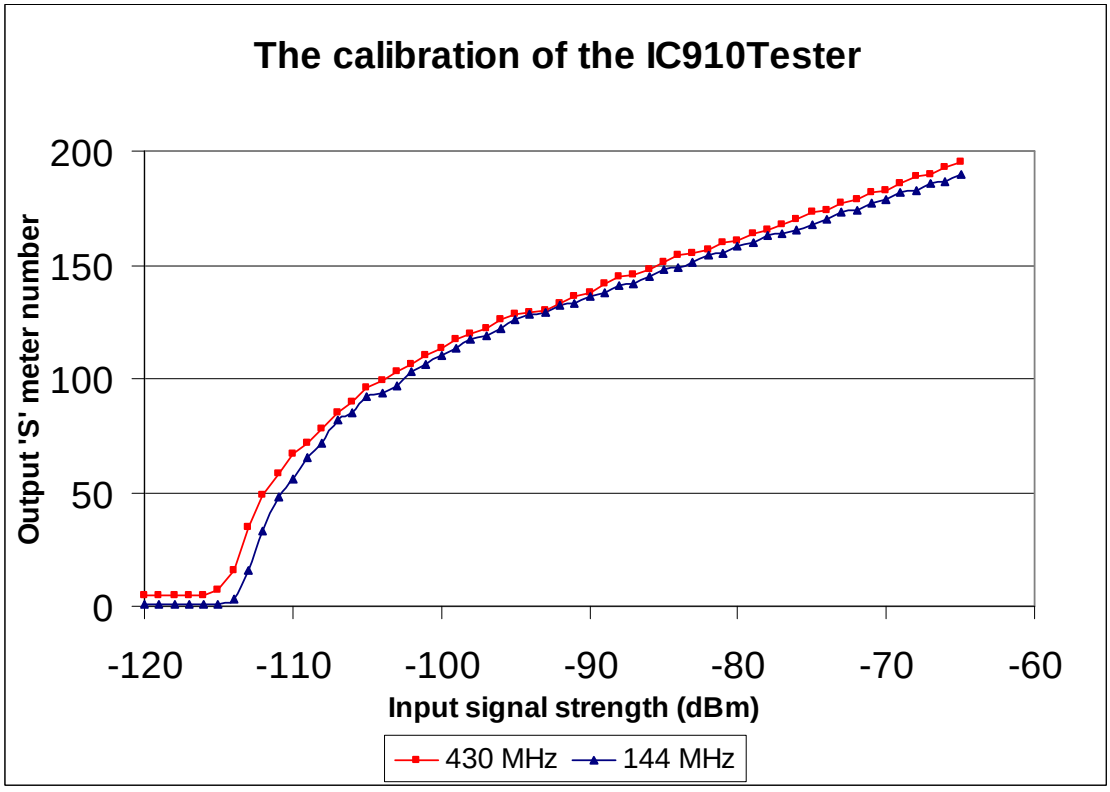

Figure 4.2 The dependence of the S-meter numbers obtained via the Icom Communications Interface on the signal level at the antenna input of the IC910H transceiver

The behavior of both UHF and VHF inputs is fairly similar. This is not very surprising, because the receiver has the same sensitivity in both bands, according to the manual, and after conversion to first intermediate frequency the signal passes the same circuitry. As seen from Figure 4.2 the relation between the input signal strength (in dBm) and output 'S'-meter readings is not linear. These values start increasing at around -115 dBm, which

is in accordance with the liquid crystal display of the transceiver. The values fluctuated quite a bit in the range up to -110 dB, because the signal strengths were comparable to the noise floor of the receiver. The recorded values in this low range were the averages of the fluctuations. Thus signals above about -110 dB can be expected to be fairly accurate, perhaps ±1dB, if one neglects the uncertainty of the absolute calibration of the signal generator, which is used equipment and has not been recalibrated very recently.

4.3 Measuring the Pre-Amplifier Gains

The actual gain of the pre-amplifiers was measured in the following manner. The Marconi 2022 signal generator was taken to the roof right in front of the antennas. A short piece of wire was inserted into the signal generator's output socket to act as an antenna. A power level of -20dBm was set up. The test was carried out for both the SP-7000 and SP-2000 pre-amplifiers, the frequencies used were 437 MHz and 145.9 MHz respectively. The pre-amplifiers were switched on and off and the resulting signal level was recorded with the already calibrated IC910Tester software.

The measurements confirmed the manufacturer's specification that by default the pre-amplifiers were set at 20±1 dB. For SP-7000 the noticed signal change was between 20 and 20.5 dB, and for SP-2000 it was between 19.8 and 20.5 dB.

4.4 Satellite Signal Strength Measurements

Besides Compass-1, XI-IV and XI-V that were observed in Chapter 3, another Japanese cubesat Cute-1 from Tokyo Technical University was also monitored here. The beacon transmitter power for Cute-1 is again 100 mW and the maximum gain of the λ/4 monopole antenna is 2 dB (Nakaya, 2004).

As the transceiver's serial port was under control of the IC910Tester, it was not possible to use Ham Radio Deluxe for automatic Doppler shift tuning this time. The Doppler shift tuning was done manually instead. This turned out to be quite successful and no significant signal losses seemed to occur. When the satellite was approaching the maximum frequency increase was 10 kHz and for receding satellites the actual frequency was 10 kHz lower from the nominal frequency value. During the pass the frequency was

decreased in 1 kHz steps according to the tone of the signal. As the bandwidth of the receiver in CW mode was 2.3 kHz, a 1 kHz tuning step was precise enough.

The distance to the satellite was recorded manually with 1 minute intervals from the Nova for Windows software. As the IC910Tester recorded the UTC time automatically for each measurement it was later possible to relate the signal strength and distance to the satellite for every datum.

4.4.1 The Results

The automated data capturing method provided much more detailed information about the signal behavior than the manual recording discussed in Chapter 3. A XI-V pass is presented on Figure 4.3.

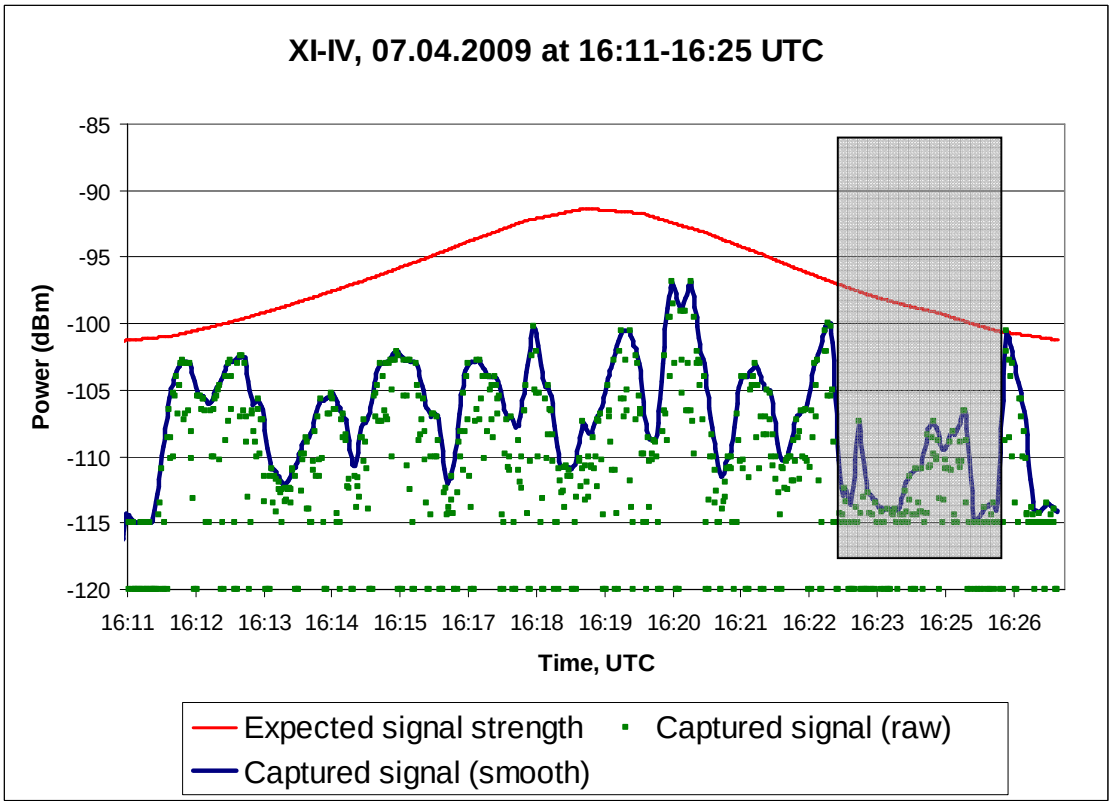

Figure 4.3 The XI-IV pass recorded with the ISU Ground Station on 7 April 2009, at 16:11 to 16:27 UTC, AOS az. 146.3º, LOS az. 350.9º, max. el. 49.7º.

The raw data included measurement points between two Morse beeps, i.e. during the times the satellite transmitter was off. An envelope curve was calculated to extract the transmitted data. This was done by taking the maximum of seven adjacent neighbors (the

current one, plus three each side) and then applying a short-period seven unit span averaging to obtain a smoother curve. On later charts only processed data is displayed to keep the figures clearer.

Here the measured signal is by about 5 dB weaker than the calculated values, and the curve is generally flatter than expected. The difference between expected and observed signal values is greater at shorter distances (higher elevation angles). The same effect could also be observed in many passes and it is further discussed in the following sections. Furthermore, the detailed data allows deriving some more information about the satellite: measuring the distance between neighboring peaks one can estimate the tumbling rate of the satellite. For the current XI-V pass the tumbling period seems to be about 1-1.5 minutes. It is also important to mark that the rotator executed a full turn during this pass between 16:23 and 16:25 (marked with a grey box on the figure, because the satellite passed through the 0º azimuth. The rotator full turn is clearly remarkable on the chart with the lower power values there, but even from the opposite direction the antennas collected up some signal as it was possible to hear Morse code through the noise.

In the following the results are displayed and observations discussed. The signal strengths are plotted against the range of the satellite. For each pass also the maximum elevation, acquisition of signal (AOS) azimuth and the loss of signal azimuth (LOS) are given. As the orbital altitude is very similar for all of the satellites then the following elevation angles correspond to the certain distances: 2800 km – 5º, 2400 km – 10º, 2000 km – 15º, 1600 km – 25º, 1200 km – 40º, 900 km – 60º.

Passes of Cute-1

A total of 4 Cute-1 passes were recorded with the IC910Tester, the 3 most interesting ones are presented here (Figure 4.4 to Figure 4.6).

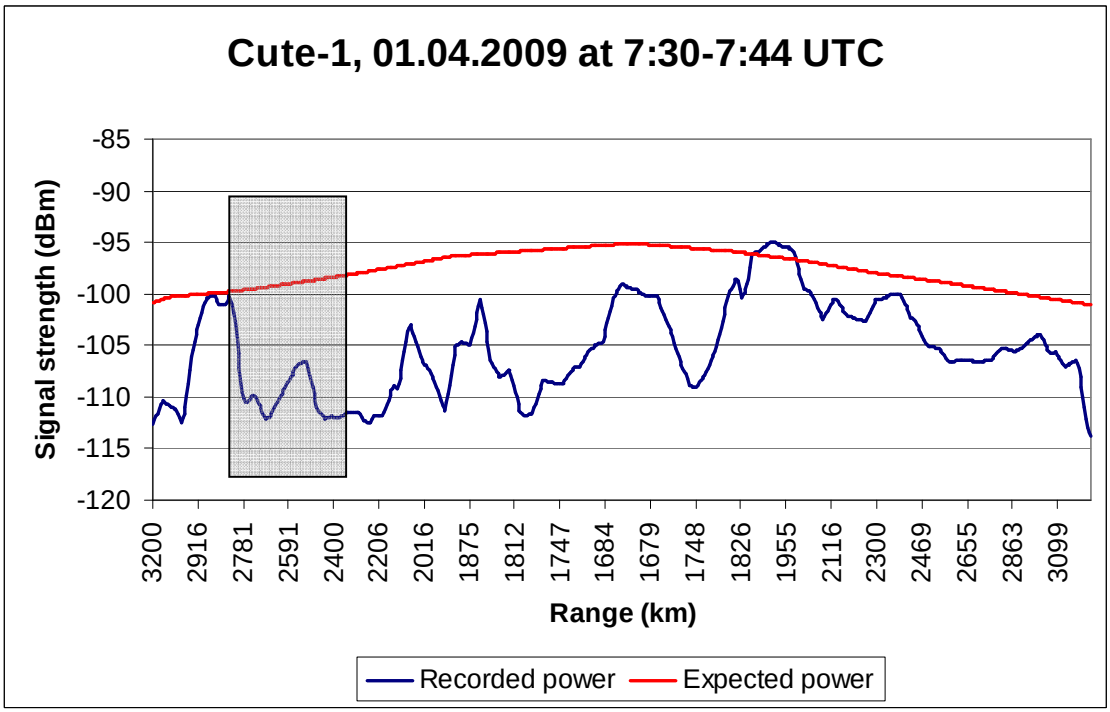

Figure 4.4 The Cute-1 pass recorded with the ISU Ground Station, AOS az. 4.9º, LOS az. 240º, max. el. 23º. The grey box marks the period when the rotator did a full turn.

The Cute-1 pass depicted on the Figure 4.4 gives a plenty of information. The signal changes over time quite a bit – being from very close to the calculated power near distances 2900 km (approaching) and 1900 km (receding), but sometimes the recorded power is up to 15 dB lower than the expected one. Besides that the signal is generally weaker when the satellite is approaching compared to the period when the satellite is receding from the Ground Station. But it is important to remark that for this particular pass the rotator executed full turn between distances 2800-2400 km (approaching), because the satellite went through 0º azimuth. Then the antenna was pointed away from the correct direction for about 2 minutes, which partially explains the weak powers during the satellite's approach.

On Figure 4.5 is given another Cute-1 pass on 7th April 2009. Here the mid-region of the pass and the receding branch follows the calculated curve behavior quite nicely, but the signal level is up to 5 dB stronger than expected for some reason.

It is interesting to remark that for this pass the signal strength varies with almost constant period of a little less than 1 minute. Besides that the approaching side is again weaker,

but here again some rotator problems deform the picture. The elevation controller hung up and the elevation rotator pointed the antenna towards the horizon even when the satellite was higher up the sky. The problem was finally recovered at 2000 km range (approaching), but the signals remained still weaker until 1500 km range (approaching), the reason of which is not clear yet.

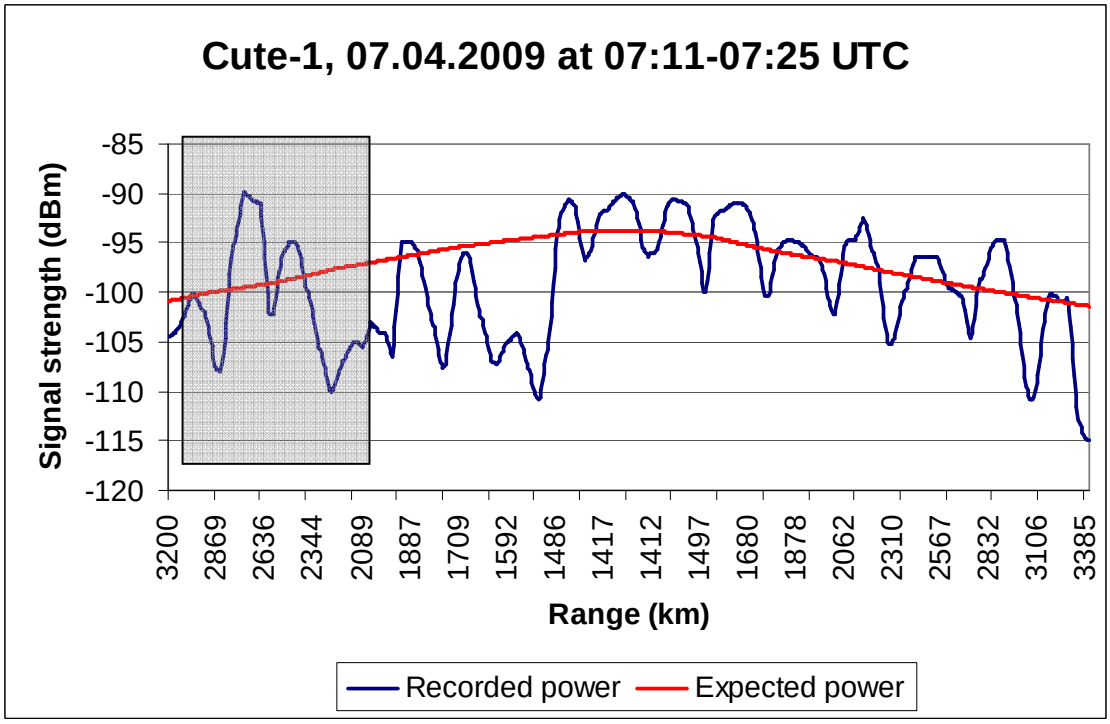

Figure 4.5 The Cute-1 pass recorded with the ISU Ground Station, AOS az. 7º, LOS az. 227.9º, max. el. 31º. Grey box marks the period when the elevation rotator was stalled on the horizontal position.

At one instant – at a distance of about 2700 km on the approaching side the recorded signal is as much as 9 dB higher than expected!

On another Cute-1 pass (Figure 4.6) recorded on the same day the captured signals follow the calculated values quite closely again. Most of the peaks are almost on the line, except the two peaks both sides, which exceed the calculations with about 6 dB. No significant signal strength difference between approaching and receding side is present here, as it was on the previous Cute-1 passes.

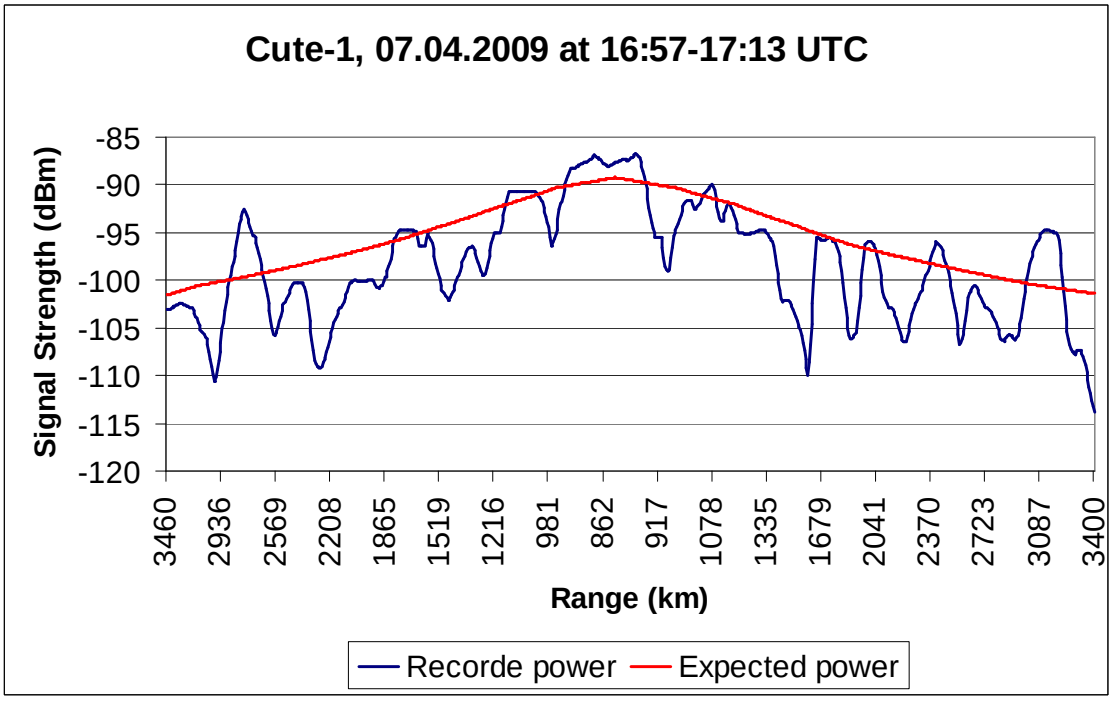

Figure 4.6 The Cute-1 pass recorded with the ISU Ground station, AOS az. 167.1º, LOS az. 344.9º, max. el. 78.3º.

The chart depicted above is very valuable, because it was a nearly over-head pass (elevation up to 78.3º) and no rotator problems were encountered.

The signal was especially strong at lower elevation angles, which is clearly seen from the two symmetrical peaks at both ends. On these cases the recorded signal was up to 7 dB stronger than calculated, the respective distances were about 2700-3100 km, which corresponds to elevation angles 2º - 6º.

Passes of Compass-1

A total of 3 Compass-1 passes recorded on the 1st and 7th April 2009 are presented in this section.

On the first Compass-1 pass (Figure 4.7) one sees the Morse code bursts separated by the 3 minute pauses – a familiar behavior of Compass-1 already described in Chapter 3. The two border bursts agree quite nicely the calculated signal values (difference only about 3 dB), while the middle one is about 7 dB lower than expected. Because of the short burst of the signals, it was very difficult to estimate the tumbling properties of the satellite.

Besides the major transmission bursts, one can also notice some minor peaks between them. These peaks are actually not noise, during the pass it was possible to hear very short Morse tone beeps, like a “leakage transmission” had occurred.

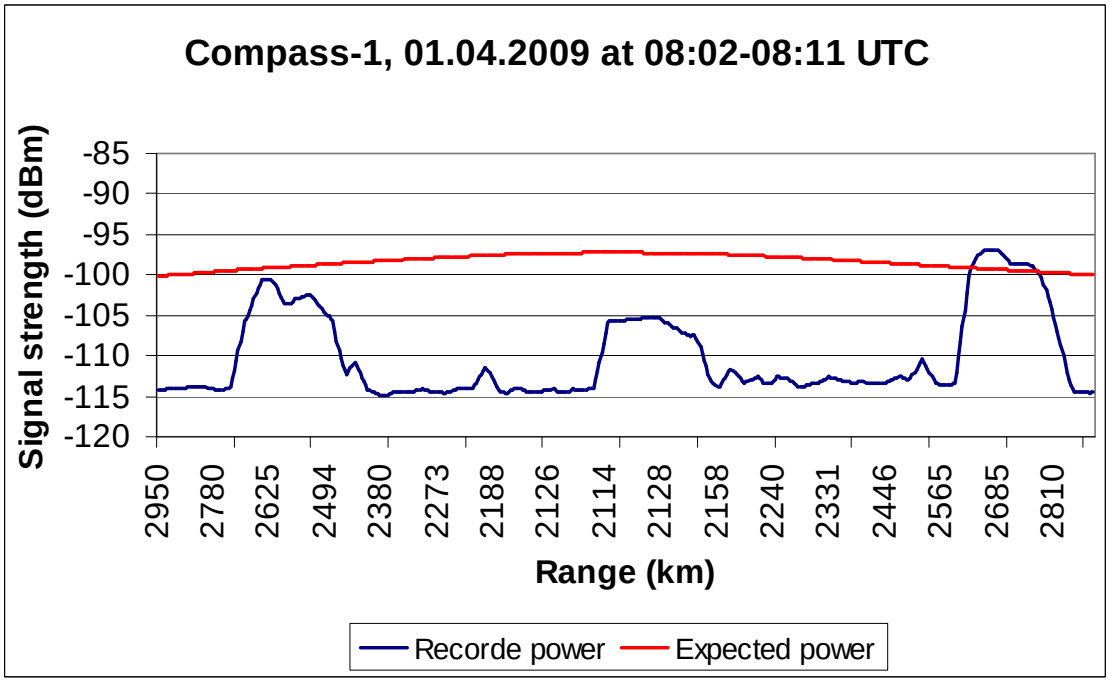

Figure 4.7 The Compass-1 pass recorded with the ISU Ground Station, AOS az. 35º, LOS az. 134º, max. el. 9º.

On the next Compass-1 pass (Figure 4.8) something unusual for Compass-1 seems to have happened. The satellite transmitted continuously and no 3 minute interval pattern was detected. For this pass no rotator problems occurred, hence all the changes in signal strength must have a different explanation. Here again the approaching side signal was significantly weaker (5 dB or more) than the ones of the receding side, which is in excellent agreement with the predictions. A similar effect was also noticed for the first two Cute-1 passes (Figure 4.4 and Figure 4.5). Besides that the receding side of the power curve follows quite nicely the expected values only some interruptions with weaker values occur.

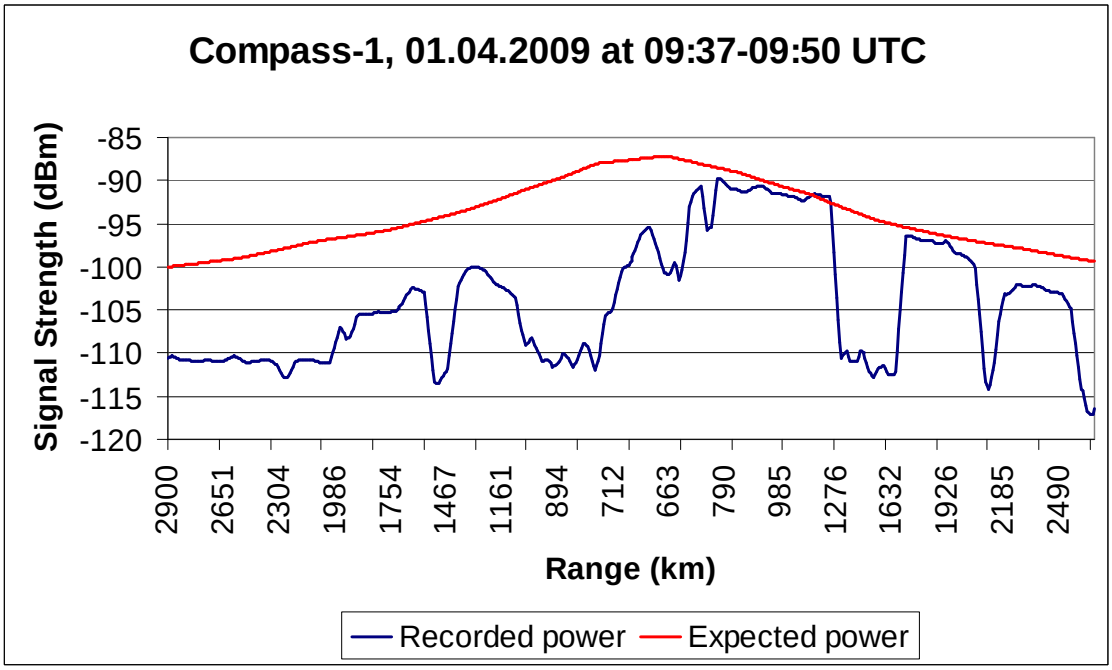

Figure 4.8 The Compass-1 pass recorded with the ISU Ground Station, AOS az. 14º, LOS az. 192º, max. el. 77º.

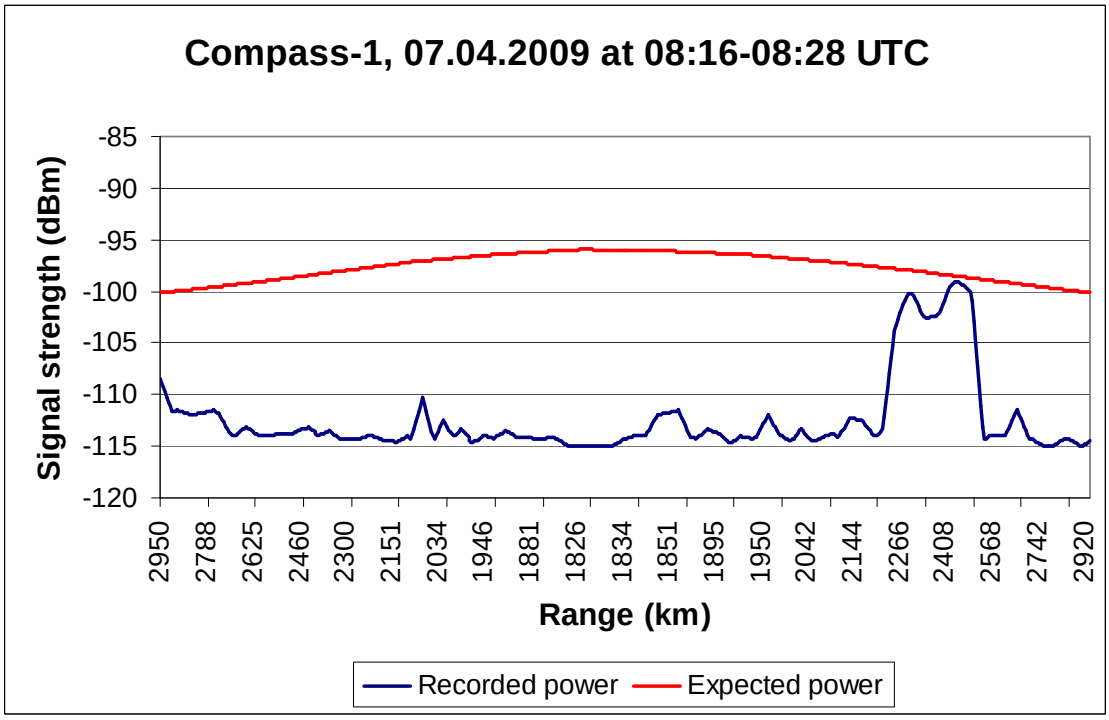

Figure 4.9 The Compass-1 pass recorded with the ISU Ground Station, AOS az. 31º, LOS az. 145º, max. el. 13º.

The last Compass-1 pass (Figure 4.9) showed another unexpected picture: During the 12-minute pass only one Morse burst occurred while there should have been three. Apart from that the signal level of the only Morse burst was very close to the calculated values (difference only 1-3 dB which is near the precision limit of this work). It is important to mark that no rotator errors or other technical problems were noticed during this pass. Hence it is very likely that there might be something wrong with the spacecraft.

Passes of XI-V

A total of 5 XI-V passes were recorded with the IC910Tester. The three most interesting and un-corrupted ones are presented here.

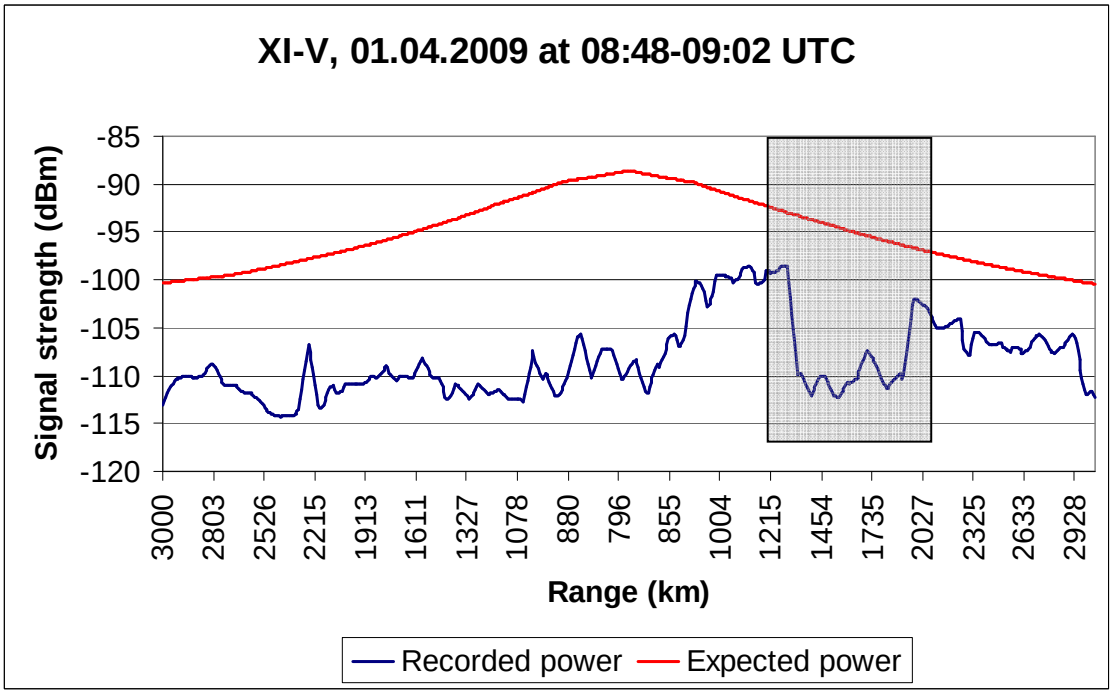

Figure 4.10 The XI-V pass recorded with the ISU Ground Station, AOS az. 156.5º, LOS az. 348.9º, max. el. 67.5º.

The first XI-V pass is depicted on Figure 4.10. This near-overhead pass – maximum elevation 67° - shows a very weak signal during approach, about 10 dB or more less than predicted. The Morse code could clearly be heard during this time. During the receding part, a substantially stronger signal was obtained, only 5 dB below expectations. Between distances 1300-1800 km, the azimuth rotator went through a full turn from 0° to 360°. This resulted in a drop of the signal to the noise floor at -110 dBm (marked with a grey

box in the figure). Except for this interval, the signal on the receding part appeared to follow the predicted curve, albeit lower by 5 dB.

Another XI-V pass – recorded on the same day is presented on Figure 4.11. In this pass of relatively low elevation the signal strengths are closer to the calculated values, differing by as little as 1dB, but still some relative signal weakening at the approaching side seems to be present (5dB). The peak value occurs is located at the receding side at 2600 km range, which corresponds to about 5º elevation angle. The XI-V beacon transmits continuously like the Cute-1 and hence the signal strength variations are observable during the whole pass. The fluctuations here are much lower amplitude and shorter period (about 20 s) than the ones observed on Cute-1 and XI-IV.

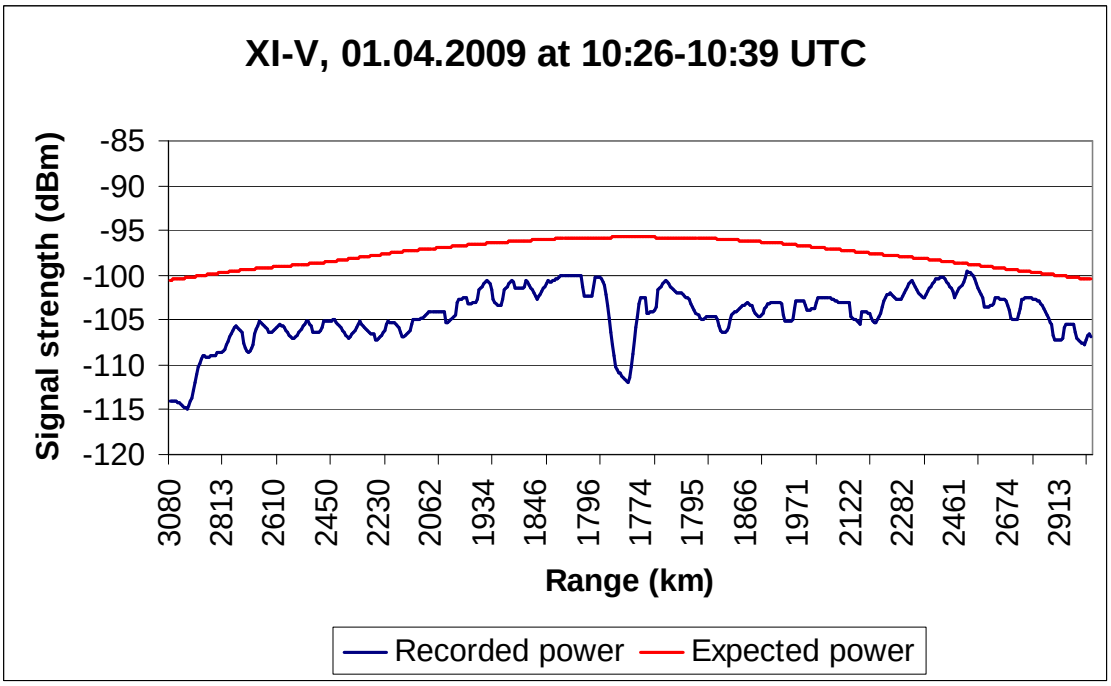

Figure 4.11 The XI-V pass recorded with the ISU Ground Station, AOS az. 210.1º, LOS az. 331.8º, max. el. 16.8º.

The last XI-V pass presented here (Figure 4.12) is free from any known Ground Station problems, no rotator full turns or errors in rotator behavior were noticed. The receding side follows the expected behavior quite nicely, but the captured signal is 4-10 dB weaker than calculated values and the signal drops somewhat faster with distance than expected. This pass is another example for the signals being weaker when the satellite is approaching.

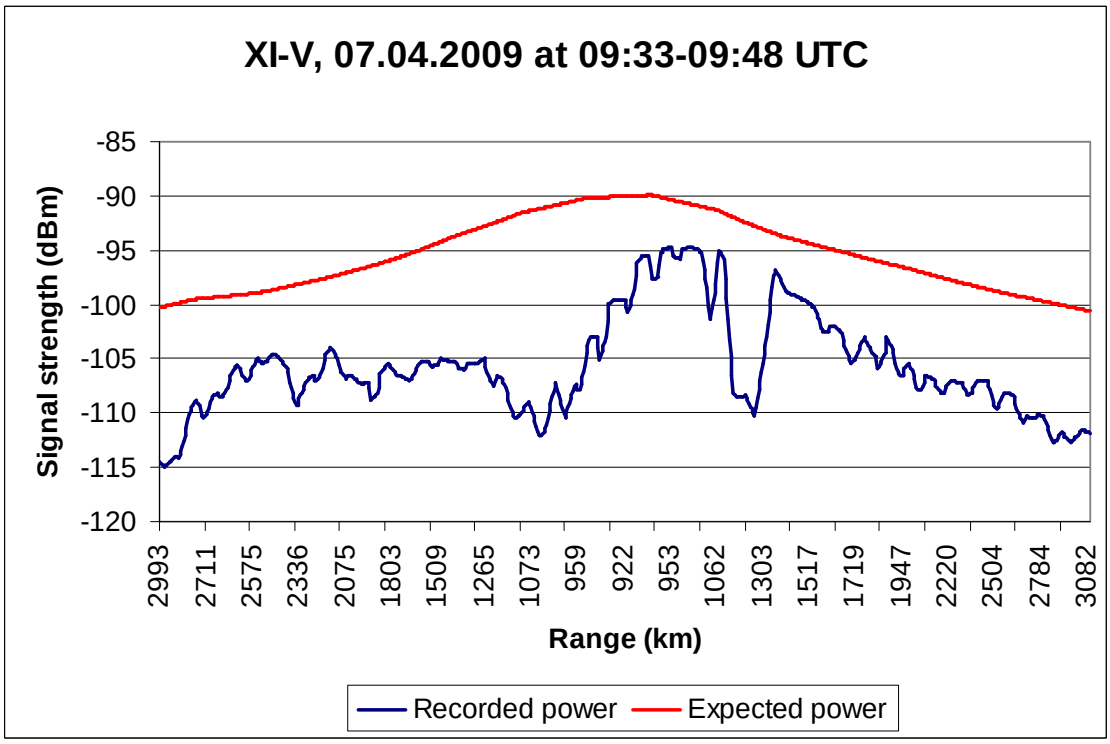

Figure 4.12 The XI-V pass recorded with the ISU Ground Station, AOS az. 180.6º, LOS az. 341.9º, max. el. 47.2º.

4.5 Interpretation of Results

The most important result of the work is the fact that in general all the measurement results are very close to the calculated values. The satellite transmitting period peaks lay usually no more than 3 dB off from the predicted powers, especially good examples are passes depicted on Figures 4.4, 4.6, 4.7, 4.8. This means there are no big errors in the ISU Ground Station and satellite transmission parameters calculations.

Two known imperfections of the model are the approximation of the atmospheric losses and signal strength variations due to tumbling of the satellite (discussed later in this Chapter). The atmospheric losses are estimated to be constantly 1 dB (see section 3.4). This is quite true for elevation angles 5º - 90º, but for extra low elevation angles the losses are actually a bit greater: 4.6 dB for 2.5º and even up to 10 dB for 0º (Ippolito, 1986). Even though the atmospheric attenuation close to horizon is quite strong, taking this effect into account will not make the model much better, because the strong attenuation is only present for very short time after AOS and right before LOS.

4.5.1 Tumbling of the Satellites

The observed signal fluctuation rates and amplitudes of the satellites are given in Table 4.1. As Compass-1 transmits in non-continuous mode for the most of the time, it was harder to determine amplitude and period of any fluctuations. The Compass-1 values given in the table are derived from the tops of separate transmission bursts.

Table 4.1 The satellite signal strength fluctuations.

Satellite	**Signal fluctuations period**	**Signal fluctuations amplitude**
XI-IV	1 - 1.5 min	5 – 10 dB
Cute-1	1 min	5 – 10 dB
Compass-1	30 s	1-3 dB
XI-V	20 s	2-3 dB

The Cute-1 and XI-IV the signal strength fluctuations are more clearly observable than on other satellite. The amplitude of these fluctuations is deeper, the period is longer and they seem to be more regular than for Compass-1 or XI-V, where most of the fluctuations have lower amplitude and the behavior seems to be more irregular.

Explanation

One possible explanation for the signal strength variations is the tumbling of the satellites. That results in random pointing of the satellite antenna and hence the actual gain for a certain moment could be much lower than the maximum gain.

For checking if the tumbling is the reason for the signal fluctuations the status of the satellites attitude controls was investigated. The Compass-1 team confirmed that their detumbling mechanism - a 3-axis magnetometer - is working properly (Piepenbrock, 2009). Hence the short period 1-3 dB fluctuations on Compass-1 transmission bursts must have other reasons than the tumbling of the satellite.

The Cute-1 team confirmed that their satellite does not have an attitude control system at all (Kawakubo, 2009). So the most likely reason for the clear signal fluctuations is the tumbling of the satellite.

The XI-IV and XI-V team confirmed via e-mail that, based on their last telemetry information in November 2008, both satellites' detumbling mechanisms were working (Komatsu, 2009). This might be still true for XI-V, which signal does not fluctuate with great amplitude. The older XI-IV (launched in 2003) high amplitude signal strength fluctuations that are very similar to the Cute-1 signal behavior, which does not have attitude control, indicate that the attitude control of XI-IV might be out of order.

Besides the attitude control status of the satellites it is interesting to remark that Cute-1 beacon signal is transmitted via a λ/4 monopole, while all the other satellites use λ/2 dipole. The directional patterns of these two antennas are given on the figure below. They could partly explain the deep amplitude fluctuations of Cute-1 as its beam width seems to be narrower.

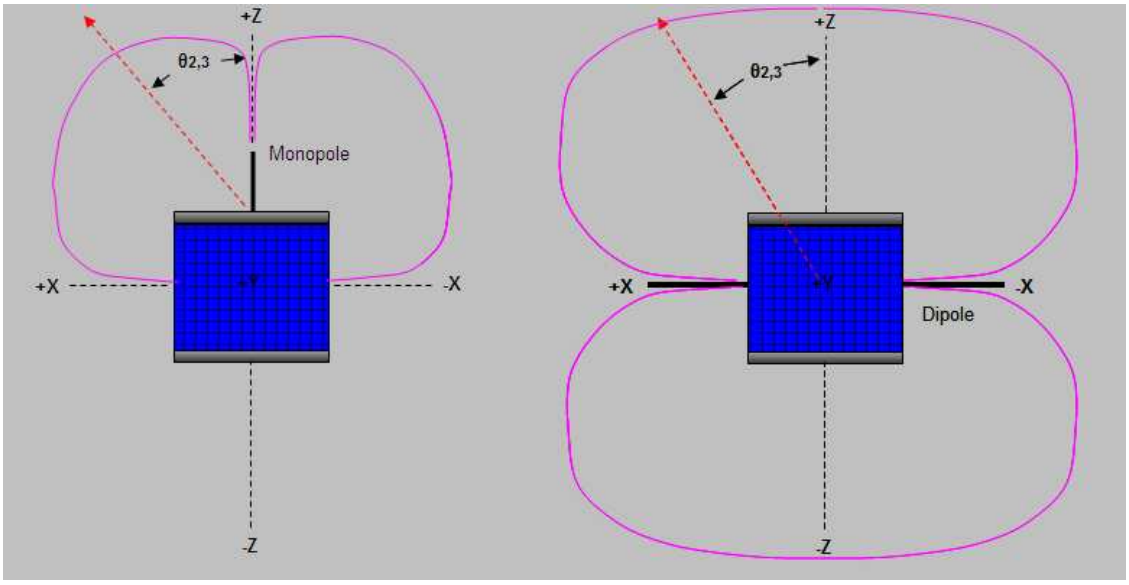

Figure 4.13 The λ/4 monopole directional pattern compared to the λ/2 dipole directional pattern mounted on cubesats (King, 2006).

Even though one can see significant differences in the directional patterns, the monopole pattern displayed is more likely true when it is mounted on an infinite ground plane. Since the real satellites are smaller (10 cm for the cubesats) than the wavelength of 70 cm for the UHF signals, the EM waves can expected to be diffracted almost equally effectively to the other side of the satellite. This means in reality the dipole and monopole directional patterns when mounted on a cubesat could be more similar than suggested in the schematic view of Fig.4.13.

4.5.2 The Differences in the Observed Signal Strengths of the Satellites

The Signals captured from Cute-1 were the strongest. The recorded power was about 3-5 dB stronger than expected for many of the peaks (Figure 4.5 and Figure 4.6). It is important to remark that all the other satellites passes gave usually power lower than expected or almost matching results with the predictions. Hence there should not be any major systematic errors in the signal strength calculations as all the satellites beacon systems have almost identical parameters.

Explanation

The most likely reason is that Cute-1 beacon output power is simply stronger than the other beacons, because the difference between actual antenna gains is very little. The λ/4 monopole and λ/2 dipole have both estimated maximum gain of 2.15 dB when mounted on a cubesat (King, 2006).

The nominal output power of Cute-1 beacon is 100mW (20 dBm), for telemetry it is 350 mW (25 dBm) (Nakaya, 2004). It is possible that the actual beacon output power is stronger – 3-5 dB higher corresponds to powers 200-300 mW.

Contrary to the estimations the Cute-1 team itself confirmed that their beacon output power is 100 mW and the maximum gain of their monopole antenna is 0 dB (Kawakubo, 2009). That means the expected power curve should be 2 dB lower instead, as the calculations in this work assumed 2 dB maximum gain for the λ/4 monopole antenna. That makes the error between expected and measured signals even greater – up to 7 dB. It would be very interesting to know, if other ground stations have also measured Cute-1 beacon power and got stronger values than the nominal 20 dBm.

4.5.3 Approaching Side Weakening Effect

When the satellite approached the Ground Station the signal was weaker compared to the captured signal when the satellite receded. This effect was observed on 6 of the total of 10 passes, for three passes no effect was noticed and for one of the Compass-1 passes (Figure 4.9) it was not possible to clearly evaluate it, because only one transmission burst occurred.

Explanation

One explanation could be connected with the elevation controller offset problem (see section 3.1.1):

- When the satellite is approaching, the elevation angle increases. Because the antenna is always pointed about 7º lower than the real elevation
- When the satellite recedes the elevation angle decreases. Hence the antenna is pointed about 7º lower than the true elevation angle.
- The elevation rotator moves with steps of about 2º, i.e. the correction in pointing is made only when the difference between the current pointing of the antenna and the actual direction to the satellite, as predicted by the NOVA software exceeds 2º. Hence the pointing error is larger (up to 9º) for an approaching satellite than for a receding one (down to 5º).
- The pointing mismatch is just because the controller turns the antenna with discrete steps. The rotators speed itself is much faster than the satellite speed across the sky. The tests showed that in worst case the elevation rotator was able to do 90º turn in 33 s and the azimuth rotator 343º turn in 105 s. While the satellite speed for elevation is about 90º in 6 minutes and for azimuth it is 180º in 6 minutes, with the peak speeds up to 20º/min for elevation and 100º/min for azimuth (computed from simulated passes). So even for a short period the rotator turning speeds are much higher than the satellite angular velocity across the sky and the pointing mismatch due to this effect can be discarded.
- Another contributor to the mismatched pointing could be the non-ideal stiffness of the antennas and the mounting frame. This means that the antennas could be actually pointed lower than the controller shows. Another contributor to this effect could be the wind that bends the antennas. To find out whether mismatched pointing could occur due non-ideal stiffness, a short test trying to move the antennas was carried out. The test gave a negative result – applying strong force to the antenna resulted in only 1-2º bending, hence the antenna system is very stiff and this effect can be discarded. Furthermore, from the experiences of a small radio telescope at ISU it is known that

wind gusts could throw an antenna in short-period shaking, but wind has not been observed to cause a deviation from its pointing lasting for a few minutes.

- The different pointing errors between 5º-9º could contribute to the signal strength difference. Causing stronger signals when satellite is receding compared to these when the satellite is approaching. The vertical HPBW of the UHF aerials system is only 15º, the 3 dB loss due to the average 7º mismatch is already taken into account. But for approaching side when the antennas could be pointed up to 9º off the losses could be much higher than 3 dB, as the gain drops quite rapidly when moving even further away from the maximum gain direction (see Figure 2.2). On the other hand when the satellite is receding, the 5º offset can cause only slightly less losses than the 3 dB for the 7º mismatch, because the gain changes little inside the HPBW. A rough estimation based on AMSAT / IARU Link Budget Spreadsheet (King, 2006) gives 2 dB losses for 5º pointing mismatch and 5 dB losses for 9º mismatch. To get know the actual numbers one should measure the actual directional pattern of the ISU Ground Station antenna system and calculate the losses based on the measurements.
- Based on this estimation the effects of the 7º pointing offset together with the pointing lag can cause up to 3 dB signal strength differences between the approaching and receding side. So this could only partially explain the phenomenon, but for some cases when the difference of signal levels between approaching and receding side was greater (up to 10 dB - Figure 4.8 and Figure 4.12), there must be other contributors to this phenomenon also.

Another explanation is connected with the ground reflections. The multipath reception of the signals in VHF/UHF region can cause up to 6 dB enhancement or down to 20 dB degradation of the signal, depending on the phase the reflected signal arrives to the antenna (McLarnon, 1997). Here it is important to remark that heavy losses (down to 20 dB) can happen only when the phasing between directly received and reflected signal is close to 180º and both are with similar powers.

The hypothesis is that from particular sides of the ISU building roof the reflected signals have arrived in opposite phase and erased the directly propagated signal. Due to coincidences this is mainly happened when the satellite is approaching the ground station.

In the table below are given all the passes parameters together with the effect strength. Described are only these regions of the passes where no rotator problems were encountered to eliminate disturbance from this factor.

Table 4.2 Summary of the presence of the approaching side weakening effect.

Satellite pass	**AOS az.**	**LOS az.**	**Max. el.**	**Signal degradation effect**
XI-IV, 07.04.2009, (Figure 4.3)	146º	351º	50º	No clear difference between approaching and receding side, deepest minimum relatively to the expected values occurred in the middle between distances 1200 km (app.) – 1100 km (rec.), corresponding el. 46º-50º and az. 93º-40º
Cute-1, 01.04.2009, (Figure 4.4)	5º	240º	23º	Clear degradation between distances 2000 km (app.) – 1750 km (rec.), corresponding el. 17º-23º and az. 335º-300º
Cute-1, 07.04.2009, (Figure 4.5)	7º	228º	31º	Strong signal degradation (about 10 dB) between distances 1800 km (app.) – 1500 km (app.), corresponding el. 20º-28º and az. 340º-315º
Cute-1, 07.04.2009, (Figure 4.6)	167º	345º	78º	No clearly suppressed signal regions, approaching and receding side almost symmetrical.
Compass-1, 01.04.2009, (Figure 4.7)	35º	134º	9º	Middle burst about 5 dB weaker than the edge ones, distances about 2100 km, corresponding el. 8º-9º and az. 75º-95º
Compass-1, 01.04.2009, (Figure 4.8)	14º	192º	77º	Deep smooth minimum at approaching side right before middle between distances 1400 km (app.) – 700 km (app.), corresponding el. 25º-70º and az. 50º -100º

Compass-1, 07.04.2009, (Figure 4.9)	31º	145º	13º	Difficult to say as only one short 1 min transmission burst occurred.
XI-V, 01.04.2009, (Figure 4.10)	157º	349º	68º	Remarkably lower signal level regions between distances 2000 km (app.) – 850 km (rec.), corresponding el. 13º-68º and az. 154º -23º
XI-V, 01.04.2009, (Figure 4.11)	210º	332º	17º	No clearly suppressed regions with longer duration.
XI-V, 07.04.2009, (Figure 4.12)	181º	342º	47º	Two suppressed regions: smooth and long at the approaching side between distances 1400 km – 900 km and a shorter steep range when receding between 1100 km 1400 km. The corresponding polar coordinate ranges are: 1. el. 25º-47º and az. 200º-260º 2. el. 36 º-24º and az. 307º-322º

There seems to be some systematic pattern in the suppressed regions with one minimum at azimuths around 320º, for a better look the situation is depicted on an azimuth plot (Figure 4.14). In addition the elevation angle seems to have to be more than 15º for this effect to occur. This indicates that due to the antenna mast height and roof edge distance, lower elevation reflections are not coming from the roof, but from the ground where surface is not so smooth, but the reflection is the stronger the smoother is the surface (McLarnon, 1997).

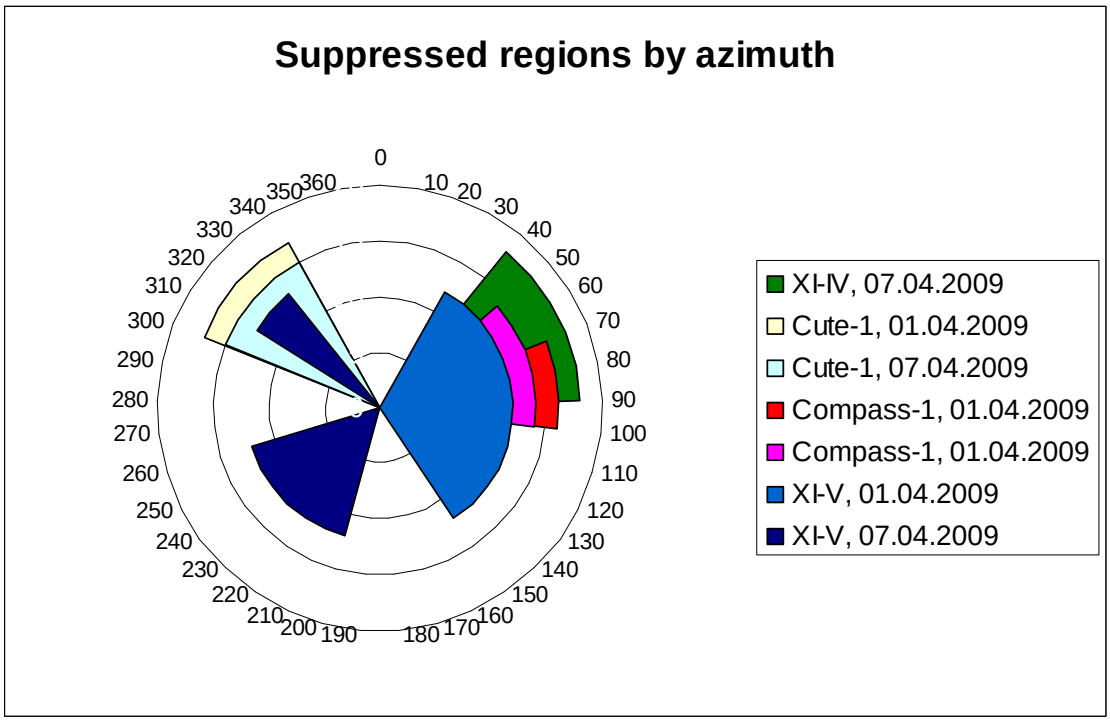

Figure 4.14. The regions were captured satellite signal was significantly lower than predicted for longer time (i. e. not the short fluctuations). Note: the different levels of the regions do not contain any information, it is just to avoid complete overlapping.

There seem to be two clearly preferred azimuth ranges, where signal suppression occurs: 300º-340º and 40º-100º. A quick survey in the data to find counter examples with signal maxima at these azimuths gave negative result.

To cause significant signal degradation the reflected signal must arrive to the antenna in close to the opposite phase. In case of equal signal amplitudes, phase difference of π can almost completely erase the signal, but even 0.75π or 1.25π phase difference can cause down to 2.4 dB degradation. So in order to this degradation mechanism to work the phase difference range of $0.75\pi \ldots 1.25\pi$ (range length of $\lambda/4$) needs to be held stable for sufficient amount of time. To better study this mechanism a sketch depicting the situation on the ISU roof is given on Figure 4.15. As the satellite is very far compared to the height of the antenna mast the directly propagated and later reflecting signals arrive almost parallel travelling the same distance. The phase difference is introduced in the very end – the direct signal travels distance x and reflected signal distance y.

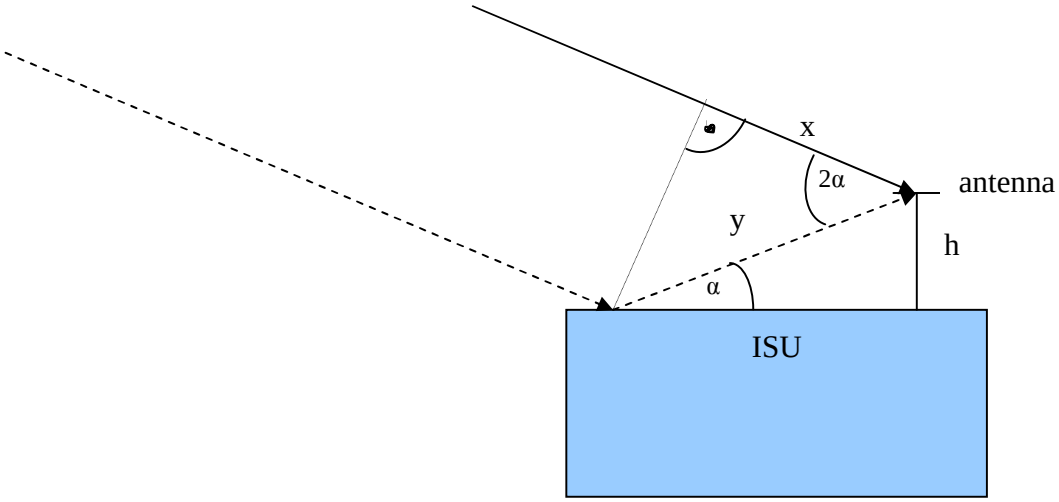

Figure 4.15 The paths of reflected (dashed line) and directly propagated (solid line) signal, α is the current elevation angle.

The propagation distances can be calculated from the following formulas:

$$y = h / \sin\alpha \qquad (4.1)$$

$$x = y \cdot \cos 2\alpha \qquad (4.2)$$

Then the path difference can be calculated directly from these formulas by subtracting y from x:

$$\Delta d = \frac{h(1-\cos 2\alpha)}{\sin\alpha} \qquad (4.3)$$

Taking account the ISU Ground Station mast height of 1.5 m and applying formula (4.3) it is possible to test whether the path difference can remain stable for sufficient elevation ranges. The results are shown on the Figure 4.16, the numbers for a 3 m mast are also given for comparison.

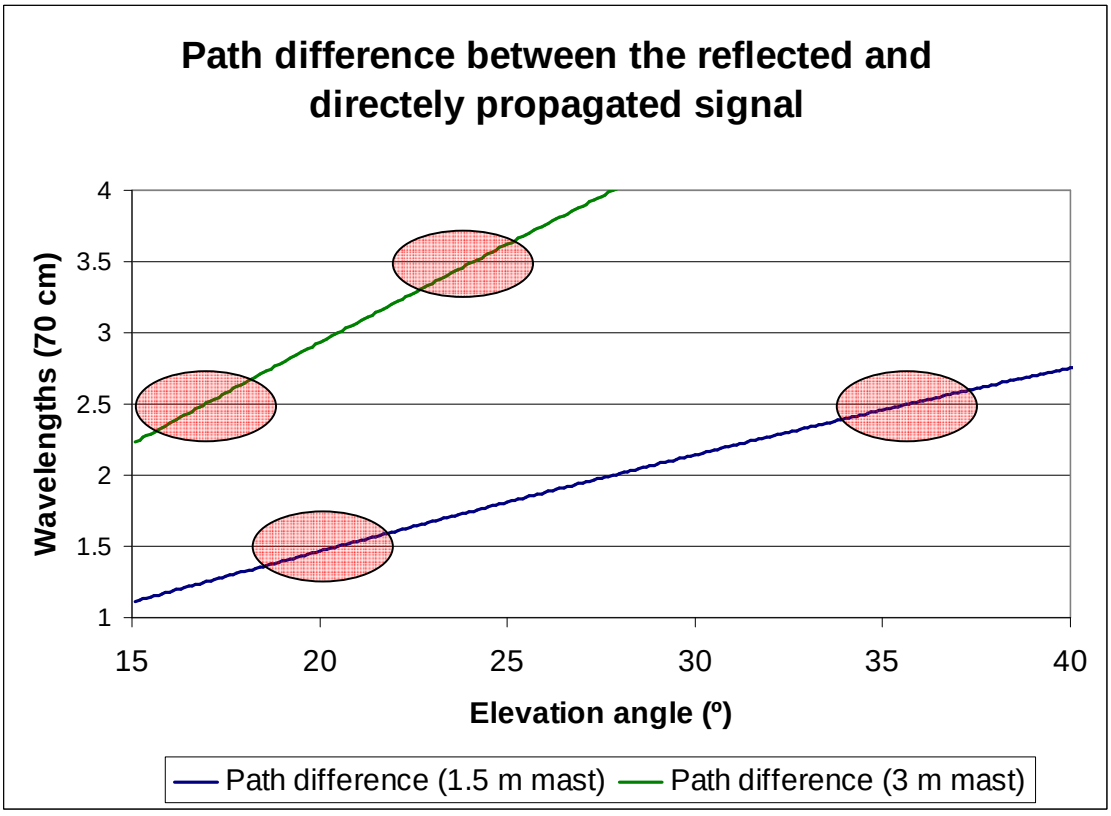

Figure 4.16 The interference minima due to path differences at certain elevation angles. Ovals mark the regions where significant (at least 2 dB) destructive interference occurs.

The phase changes linearly together with path difference, which increases when the elevation increases. Besides that it is easy to see that the higher is the mast the more frequently changes the phase of the reflected signal. For changing the phase by one λ it takes a 15º change in elevation for 1.5 m mast height. Hence to keep the phase difference within 0.75π…1.25π (path difference ranges 0.375...0.625λ, 1.375...1.625λ etc) necessary for the interference minimum, corresponds about 4º range in elevation. That means this theory cannot explain the longer lasting weakening effects (Table 4.2) with elevation changes more than 10º, because within that range the interference would have changed from minimum to maximum. The theory could still explain suppression regions where the elevation did not change so much (Table 4.2 – XI-IV pass, first two Cute-1 passes).

For further confirming or disproving the explanation one should look the ISU Ground Station antenna surroundings on the roof very carefully to explain why the reflections

could more likely occur from the directions 300º-340º and 40º-100º, but not from the others.

4.5.4 Signal Enhancement Close to Horizon

The most interesting observation is the unexpected signal enhancement at low elevation angles. The effect is clearly present on Figures 4.3, 4.5, 4.6, 4.7, being especially clear on the last pass of Cute-1 (Figure 4.6), which also very valuable because it is a high elevation pass when no rotator problems were noticed. That means the satellite signal is relatively stronger at large distances (low elevation angles) than at close distances (high elevation angles) compared to the estimated power values.

Explanation

The short distance degradation might have explanation by the roof reflections as described in section 4.5.3, but signal enhancements at low elevation angles must have other reasons.

One possible explanation for the exceptionally strong signals at low elevation angles is connected with the propagation of the EM waves. The path losses used in the received signal strength calculations (Equation (3.2)) assumes isotropic propagation as in completely empty space. In the case of satellites orbiting around the Earth this is not true – the atmosphere and the Earth itself change the propagation paths due to reflection, refraction, and diffraction (McLarnon, 1997):

- Diffraction around objects close to the direct path allows propagation behind obstacles.
- Refraction in the Earth atmosphere bends the radio wave trajectory.
- Reflections from objects on the Earth or from the atmosphere allow multipath propagation.

The diffraction effects not only allow to pass the EM waves behind the obstacles, but also change the field strength very close to the obstacle edge still in line of sight. The field change close to the obstacle edge is between 6 dB loss and 1.2 dB increase compared to the free space case (McLarnon, 1997). So diffraction alone can not fully explain the observed 5 dB power enhancements close to horizon at elevation angles 2º -6º (Figure

4.6). Reflection and refraction can cause greater changes. Possible different propagation paths are shown in the sketch below.

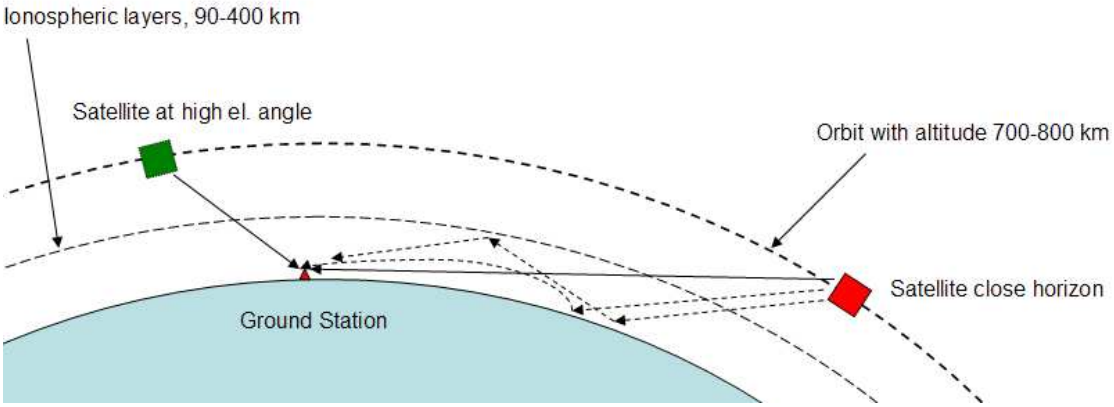

Figure 4.17 The satellite signal propagation at different elevation angles. Solid arrows depict directly propagated signal and dashed arrows signal propagation paths that include reflections and refraction.

At high elevation angles only the direct propagated waves contribute to the received signal, but at low elevation angles other propagation effects could also be present: At first the directly propagated path (solid line) is also bent a little bit along the curvature of the Earth, but this could rather decrease the signal strength, because it travels longer distance in the atmosphere and encounters higher atmospheric losses. Two indirect paths (dashed line) can be envisaged:

1. Signal is reflected at the Earth surface and then by the ionosphere, before reaching the Ground Station.
2. Signal is reflected on the ground and then it is refracted along the curvature of the Earth to reach the Ground Station.

The first path propagation is probably not very strong, because it includes two reflections with losses and especially the second ionosphere reflection is not very strong at UHF frequencies. The second path is more likely, but two conditions must be present to make it possible:

- The surface where the Earth reflection takes place must be smooth to make the reflected signal strong enough.

- The refraction index must be such that the reflected signals bend just enough to reach the Ground Station.

In normal conditions the refraction index is such that the signal propagates with arc which radius is 4/3 of the Earths radius, but the refraction index and hence the propagation arc curvature depends greatly on the atmospheric conditions. In case of particular atmospheric conditions superrefraction or subrefraction can occur. In subrefraction the propagation horizon is reduced and in superrefraction it is extended over the visible horizon (McLarnon, 1997).

4.6 Results Summary

The automatic data capturing method helped to better understand the characteristics of ISU Ground Station and the satellite signal behavior. The approaching side weakening effect discovered in Chapter 3 was confirmed and some new phenomena, like the signal enhancement close to horizon, were observed. Most of the interpretations remain still at a likely hypothesis level. For further studying the discovered behavior known problems (such as elevation rotator offset and tracking system hanging) should be eliminated and then more measurements should be done to make fair conclusions.

5 Case Study: The University of Tartu Ground Station

The University of Tartu Ground Station is one of the newest members in the GENSO network, having been set up in the autumn/winter 2008. The system has connection capabilities in two bands: VHF and UHF. The antenna system with four 70cm and two 2m antennas mounted on the Physics Department roof is depicted on Figure 5.1.

Figure 5.1 The Tartu University Ground Station antenna system mounted on the top of Physics Department building (Estcube Team, 2008).

5.1 System Overview

The component specifications according to the manufacturers data is given in the table below.

Table 5.1 The components of the University of Tartu Ground Station.

Component	Manufacturer and model	Gain or loss
70 cm UHF crossed Yagi-Uda antenna	Wimo WX 7036 Kreuzyagi 70cm 2x18-Ele	16.15 dBi (single antenna)
2 m VHF crossed Yagi-Uda antenna	Wimo WX 214 Kreuzyagi 2m 2x7-Ele	12.15 dBi (single antenna)
UHF pre-amplifier	SSB Electronic SP-7000	20 dB
Transmission cable	Ecoflex 15	6.1 dB /100 m (432 MHz, 20°C) 3.4 dB /100 m (144 MHz, 20°C)

The connection diagram is depicted below.

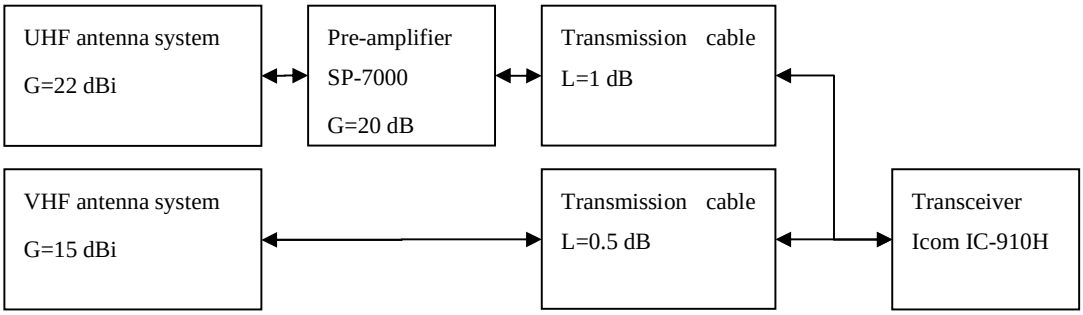

Figure 5.2 The component connection diagram.

Detailed system description is given in Urmas Kvell's Bachelor's Thesis about the University of Tartu Ground Station Radio Connections (Kvell, 2009).

5.2 The Analysis Method

To analyze the signal a different method was used. Instead of S-meter recording the audio file of the satellite beacon Morse code was captured. For capturing the audio the output of the transceiver was directly connected to the soundcard input of the computer, where the Audacity software was used to store the signal into a file. The file stored was a raw uncompressed waveform audio with no software signal processing to get the signal in an untouched form for later analysis.

For extracting the signal behavior from the audio file to an Excel-readable text file the JAVA software AudioMeter written by Prof. Joachim Köppen was used. The software uses waveform audio as its input and converts the information into text form while simultaneously showing the results chart on the screen. It is possible to choose both: linear and dB output, for the purpose of this work the dB output was used. A screenshot of the software is displayed on Figure 5.3.

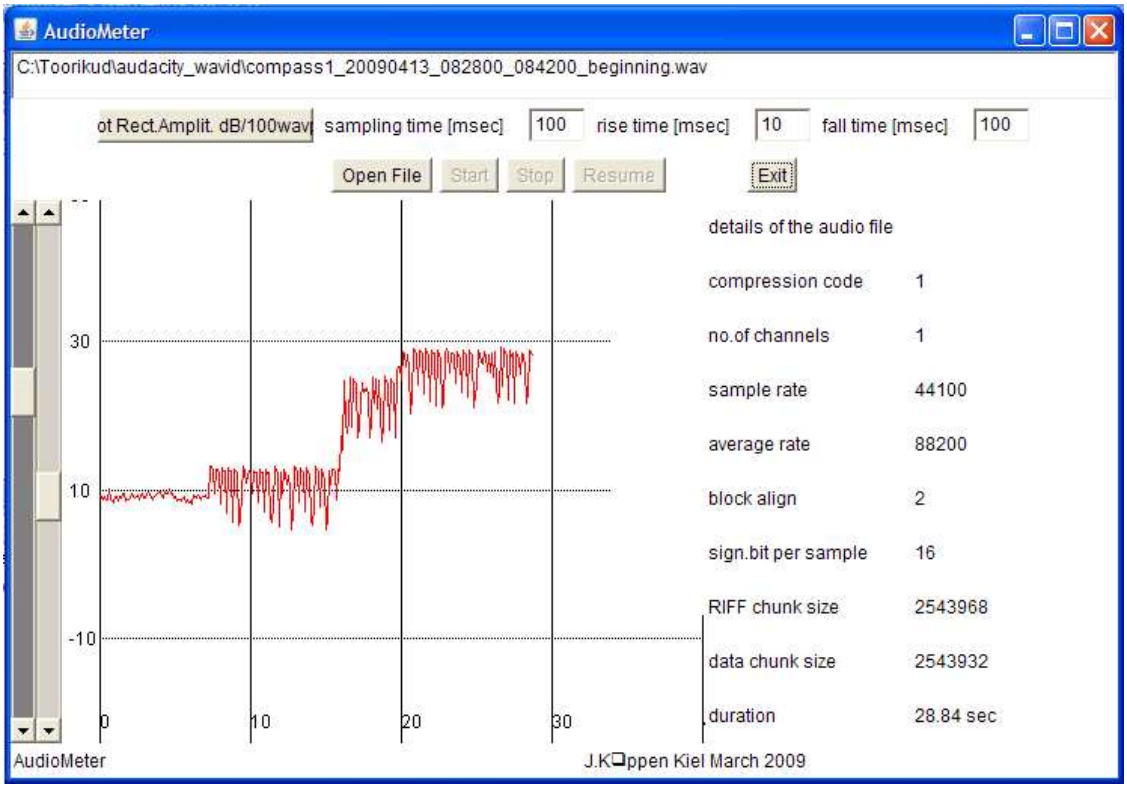

Figure 5.3 The AudioMeter software showing an audio signal output in dB form.

For processing the audio file it is necessary to choose three parameters: sampling time, rise time and fall time. The sampling time is simply the results writing interval to the file. The rise time and the fall time determine the smoothing sensitivity of the program. The software imitates a hardware filter depicted on the following figure.

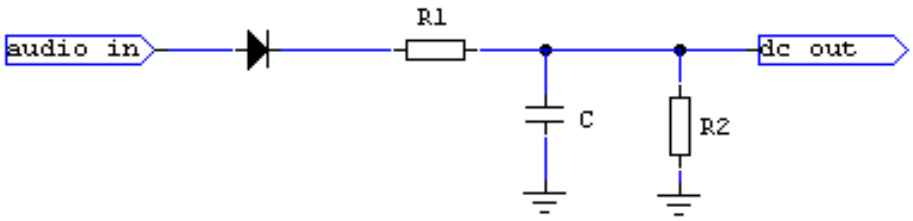

Figure 5.4 The concept diagram of the hardware filter that the AudioMeter software imitates.

The input signal is fed into a capacitor through a rectifying diode and a charging resistor R1 and the capacitor is discharged via a resistor R2. The rise time is determined by the R1 and the resistance of the diode; with a shorter rise time the capacitor charges more quickly. The fall time is determined by the discharging resistor. The shorter the fall time is the faster the capacitor can discharge and thus the shorter is the memory of the circuit. With short fall times one can follow even the shortest fluctuations in the output while longer fall time smooth out the output, acting like a low pass filter.

5.3 Sample Measurement Analysis

For a first, exploratory test a Compass-1 pass recorded on 13th April 2009 at 8:28-8:42 captured with the University of Tartu Ground Station is shown on Figure 5.5. During this pass, the signal reached a maximum strength of S9+10dB (Urmas Kvell, private communication). Thus the signal is strong enough to actuate the receiver's AGC system, which will keep the audio output nearly constant. Consequently only the weak signal part of the data can be used to check our method. The parameters for the AudioMeter were chosen 10 ms for rise time and 3000 ms for fall time, because the signal powers between the Morse code were not important for the general signal behavior.

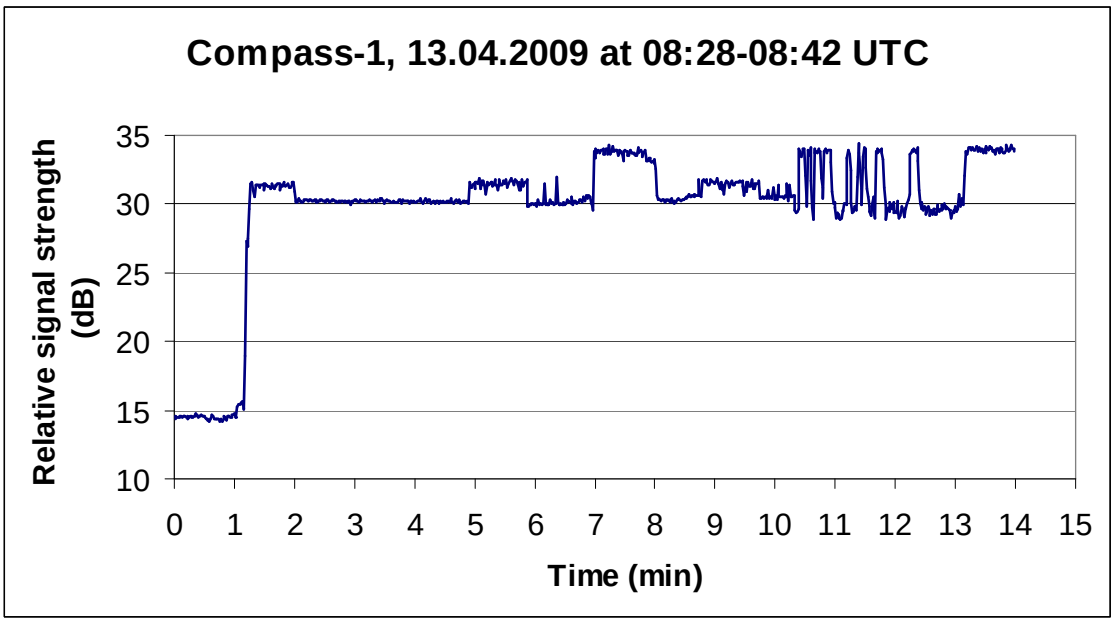

Figure 5.5 The Compass-1 pass recorded with the University of Tartu Ground Station.

In the beginning of the recording the pre-amplifier was switched off and the signal level is about 14-15 dB. Then at 1 min the pre-amplifier is switched on and one can see about 16 dB signal power increase. According to Urmas Kvell the pre-amplifier should be at its default maximum setting of 20 dB (Kvell, 2009). The discrepancy in the observed pre-amplifier gains is undoubtedly due to the action of the receiver's AGC system which lowers the gain for the stronger signals, and therefore changes in the audio level do not correspond exactly to the changes of the r.f. signal. That this already affects weak signals can be seen in Figure 5.3 which shows this audio file, but zoomed around the time of the switching-on of the preamplifier: the white noise in absence of any signal gives a higher audio signal than the noise in between the pauses of the Morse code beeps (near time = 10s). Thus, the audio analysis method cannot be used to its full potential with this data set.

When listening the audio recording there are three clearly readable Morse code bursts at ranges 1-2 min, 5-6 min and 9-10 min, separation interval 3 min – a common behavior of Compass-1. These bursts are about 3 dB above the noise background. Besides that it is possible to hear very short beeps after the 5-6 min and 9-10 min Morse code bursts. A similar behavior was also noticed with the ISU Ground Station in April 2009 when listening the Compass-1 beacon. It sounds like the Morse code data flow is leaking to the

transmitter at the time it is not supposed to transmit (the regular 3 min pauses between transmission bursts). Since 10 min it is possible to hear some strange periodic sounds alternately with rushing noise. The periodic sounds suggest that the transceiver was switched to receive the telemetry of Compass-1 from a different frequency. Unfortunately a proper description protocol about the pass was not available, that could explain what exactly was captured.

After the pre-amplifier is switched on, there is only a slight difference in the audio levels when the satellite was transmitting Morse code and when it was not transmitting. This does not mean that the signal to noise ratio was only 2-3 dB, but it is due to the working of the automatic gain control (AGC) of the Icom 910H transceiver. To better illustrate the situation an Audacity screenshot from the end of the last Morse transmission range is given on Figure 5.6 below.

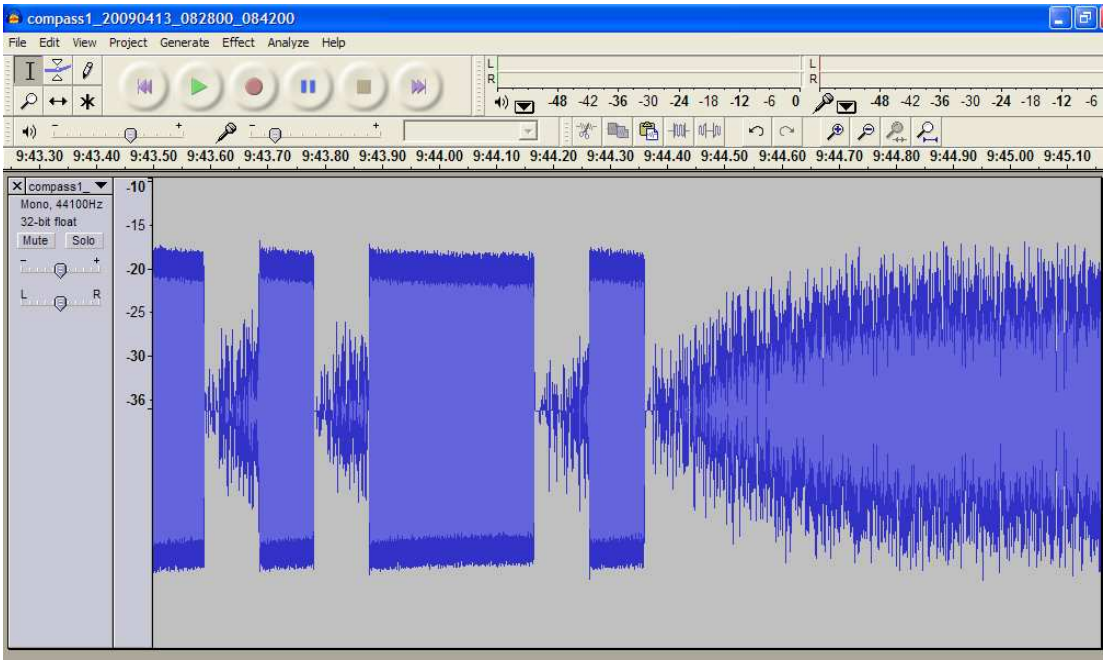

Figure 5.6 A screenshot from Audacity showing a short range of the Compass-1 audio file.

The Morse beeps are clearly noticeable as constant tones (forming the letter ‘F’). After each beep, the noise starts to grow gradually, as the AGC system tries to increase the gain back to its maximum value. When a new beep begins, the gain is rapidly reduced, to keep the audio level constant. After the last Morse beep the AGC increases the gain again, but as no new Morse beeps occur, it can reach maximum gain after about 0.5s and the audio

noise reaches a level almost as strong as the Morse signals themselves, but substantially stronger than the audio noise heard in the intervals between the Morse beeps. This is what is seen in Figure 5.3 in the behavior of the amplitudes. Hence as long as the AGC system is operating, measurement of the audio output allows only an estimate of the strength of the r.f. input.

The analysis of the sample audio file captured with the University of Tartu Ground Station demonstrated that nonetheless it is possible to roughly estimate the satellite pass signal behavior even with such an indirect method. Obviously, in order to test this method more deeply, the analysis should be repeated with a data set obtained with signals sufficiently weak for the AGC to remain inactive. Application of this method would be limited to signals sufficiently weak, so that the AGC system does not act. This would allow stations without preamplifier or high-gain antennas or during times of inoperable preamplifiers or damaged antennas to perform measurements of the signal strength and thus obtain valuable data on the satellite's current status.

6 Conclusion

The goal of the work was to try to obtain quantitative measurements of satellite signal strengths, using the ISU Ground Station, thus exploring the capabilities of the Ground Station equipment as well as verifying in a quantitative way that the equipment works according to the specifications. This involved development of the techniques and methods, which could later be used for further studies and for student projects at ISU. The gained experience is also very valuable for future developments of the University of Tartu Ground Station.

The most important results of the work are:

- The Icom IC-910H calibration confirmed the previous test results (Flechtner, 2001), the difference with current measurements was only up to 3 dB. So one who lacks a signal generator can use these results as an etalon.
- The S-meter capturing software IC910Tester written by Prof. Joachim Köppen proved to be very useful and reliable for recording satellite signal strengths. The software could be used in future studies of similar topics.
- The measurements at UHF band did show compatible results with calculations. The recorded signal peaks were typically on line with calculations or no more than 3 dB lower.
- The satellite signal measurements at VHF band were unsuccessful, an extensive noise was discovered at 145.900 MHz around the ISU Ground Station. The noise was mapped and quite clear relation between noise power and presence of close buildings was discovered.
- Cute-1 cubesat beacon signals were the only ones that gave systematically 3-5 dB higher powers than calculated from the satellites specification.
- At some passes a significant signal enhancement was discovered when satellite was close to horizon (2º-6º elevation angle). It is possibly due to UHF signal propagation effects, but the signal enhancement mechanism is not fully understood.

- At approaching branch the satellite signal was suppressed by down to 10 dB for most of the passes. Closer investigation revealed that it happened most frequently for azimuths 40º-100º and 300º-340º together with at least 17º elevation angles.
- Deep (5-10 dB) periodic fluctuations of the Cute-1 and XI-IV signal suggest that these satellites are freely tumbling in the space. It is known that Cute-1 does not have attitude control (Kawakubo, 2009) while XI-IV has (Komatsu, 2009). As the signal behavior of these satellites is very similar, it strongly suggests that the attitude control system of XI-IV is out of order.
- The University of Tartu Ground Station captured audio file analysis demonstrated that even with such an indirect method it is possible to roughly estimate the satellite signal behavior.

Recommendations for future works

More trials to connect the satellites at VHF band should be made. The calculations show that despite the heavy noise present at VHF wave region the expected satellite signals should still be at least 10 dB stronger. The extensive noise discovered at VHF region also needs further investigation. It needs to be answered what are the sources for this noise and whether it is possible to still get useable connections at that band.

Despite the general success in UHF band there are still many interesting unanswered questions. As the elevation controller offset was fixed shortly after the error discovery, new measurements could verify whether the approaching side weakening effect is still present, because one possible reason for that effect was the elevation controller offset. Besides that it would be interesting to see if it is possible to find any more proofs for the low elevation angle signal enhancement phenomenon and if it is possible to find some systematic patterns in the occurrence of this effect.

7 References

1. AMSAT INDIA, 2005. Hamsat Payload Information. Available from: http://www.amsatindia.org/payloads.htm
   [Accessed 12 March 2009]
2. BROWN, S., 2009. Ham Radio Deluxe. Available from: http://www.ham-radio deluxe.com/Programs/HamRadioDeluxe/tabid/88/Default.aspx
   [Accessed 13 April 2009]
3. FLECHTNER, U., DG1NEJ, 2001. IC910H – Icoms neuer VHF/UHF – Allmode-Transceiver. Funkamateur, 2001/6, p. 604.
4. IPPOLITO, L.J., 1986. Radiowave Propagation in Satellite Communications. New York: Van Nostrand Reinhold Co.
5. KING, J.A., 2006. AMSAT / IARU Link Budget Spreadsheet. Available from: http://www.amsat.org.uk/iaru/AMSAT-IARU_Link_Budget_Rev2.4.1.xls
   [Accessed 28 April 2009]
6. KOMATSU, M., (mitsuhito.komatsu@gmail.com), 18 May 2009. Re: XI-IV and XI-V. e-Mail to K. VOORMANSIK (kaupo.voormansik@masters.isunet.edu)
7. KRAUS, J.D. AND MARHEFKA R.J., 2002. Antennas for All Applications. 3rd ed. New York: McGraw-Hill.
8. KVELL, U., 2009. Tartu Ülikooli satelliitside keskuse raadioühendused. Thesis (BTh). University of Tartu.
9. KAWAKUBO, M., (kawakubo@lss.mes.titech.ac.jp), 23 May 2009. RE: Cute-1 attitude control. e-Mail to K. VOORMANSIK (kaupo.voormansik@masters.isunet.edu)
10. LEE, S., 2008. CubeSat Design Specification. California Polytechnic State University. Available from: http://cubesat.atl.calpoly.edu/media/CDS_rev11.pdf
    [Accessed 25 May 2009]
11. M2 ANTENNA SYSTEMS, 2008. 436CP30 Polarized Yagi Specifications. Fresno. Available from: http://www.m2inc.com/products/uhf/70cm/436cp30.html
    [Accessed 13 April 2009]

12. M2 ANTENNA SYSTEMS, 2008. 2MCP14 Polarized Yagi Specifications. Fresno. Available from: http://www.m2inc.com/products/vhf/2m/2mcp14.html [Accessed 13 April 2009]
13. MCARTHUR, D., VK3UM, 2002. The VK3UM Radiation and System Performance Calculator. Available from: http://www.sm2cew.com/rpc.pdf [Accessed 18 April 2009]
14. MCLARNON, B., VE3JF. 1997. VHF/UHF/Microwave Radio Propagation: A Primer for Digital Experimenters. Available from: http://www.tapr.org/ve3jf.dcc97.html [Accessed 20 May 2009]
15. NAKAYA, K. AND OTHERS, 2004. Tokyo Tech CubeSat: CUTE-I – Design & Development of Flight Model and Future Plan. Tokyo. Available from: http://lss.mes.titech.ac.jp/ssp/cubesat/paper/AIAA_TokyoTechCubeSat.pdf [Accessed 18 April 2009]
16. NORTHERN LIGHTS SOFTWARE ASSOCIATED, 2009. Nova for Windows. Jamesville, New York. Available from: http://www.nlsa.com/nfw.html [Accessed 13 April 2009]
17. PIEPENBROCK, J., (johannes.piepenbrock@gmx.de), 18 May 2009. RE: Compass-1 attitude control. e-Mail to K. VOORMANSIK (kaupo.voormansik@masters.isunet.edu)
18. PRATT, T., BOSTIAN, C.W. AND ALLNUTT, E.A., 2003. Satellite Communications. 2nd ed. Hoboken: John Wiley & Sons.
19. SSB ELECTRONIC USA, 2004. SP-6/ SP-2000/ SP-222/ SP-7000 Super Amp GaAsFET Series. Mountaintop. Available from: http://www.ssb.de/amateur/pdf/instruction-sp-dcw.pdf [Accessed 13 April 2009]
20. TERMAN, F.E., 1955, Electronic and Radio Engineering. 4th ed. McGraw-Hill.
21. TIMES MICROWAVE SYSTEMS, 2008. LMR-600 Coxial Cable Specifications. Wallingford. Available from: http://www.timesmicrowave.com/content/pdf/lmr/28-31.pdf [Accessed 16 April 2009]

22. TOLYARENKO, N. 2008. *Principles of Space Telecommunications*. International Space University. 23 September 2008.

23. TOLYARENKO, N. and ESTEVES, P. 2008. *Link Budget.* International Space University. 7 November 2008.

24. TU DELFT CUBESAT TEAM, 2008. Radio Amateur Information. Available from: http://www.delfic3.nl/index.php?option=com_content&task=view&id=63&Itemid=107 [Accessed 12 March 2009]

25. UNIVERSITY OF AACHEN CUBESAT TEAM, 2004. Phase B Documentation. Available from: http://www.raumfahrt.fh-aachen.de/downloads/Phase_B.pdf [Accessed 14 February 2009]

26. UNIVERSITY OF TOKYO CUBESAT TEAM, 2001. Critical Design Review. Available from: http://www.space.t.u-tokyo.ac.jp/cubesat/publication/cdr.ppt [Accessed 14 February 2009]

List of Acronyms and Variables

AGC	automatic gain control
AMSAT	Radio Amateur Satellite Corporation
AOS	acquisition of signal
CW	continuous wave
dBm	decibel milliwatt
EMF	electromotive force
G_{amp}	gain of the amplifier
GENSO	Global Educational Network for Satellite Operations
G_r	gain of the receiving antenna
G_t	gain of the transmitting antenna
HPBW	half power beam width
IARU	International Amateur Radio Union
ISU	International Space University
k	antenna efficiency factor
L_a	atmospheric losses
L_{cab}	cabling losses
LEO	low Earth orbit
LOS	loss of signal
L_p	path losses
NORAD	North American Aerospace Defense Command
PD	potential difference
P_r	received power
P_t	transmitted power
RFI	radio frequency interference
UHF	ultra high frequency
UTC	Coordinated Universal Time (Fr. Temps Universel Coordonné)
VHF	very high frequency
Θ_{HP}	half power beam width in vertical plane
Φ_{HP}	half power beam width in horizontal plane

Appendix A: S-meter calibration data

All the signal generators used were Marconi Instruments 2022.

7.1 Calibration of the IC-910H UHF input

1. test, 437 MHz, CW mode, 1. generator

S-meter (radio display)	S-meter reading (software)	input power (dBm)
0	0	-117
0	1	-116
0	2	-115
0	3	-114
1	4	-113
1	4	-112
2	5	-111
2	6	-110
3	6	-109
4	6	-108
4	7	-107
5	8	-105
6	8	-103
7	9	-101
8	9	-99
8	9	-97
9	9+10dB	-95
9	9+10dB	-93
9	9+10dB	-91
9+5dB	9+10dB	-89
9+10dB	9+20dB	-87
9+10dB	9+20dB	-85
9+15dB	9+20dB	-83
9+15dB	9+20dB	-81
9+20dB	9+20dB	-79
9+20dB	9+30dB	-77
9+25dB	9+30dB	-75
9+30dB	9+30dB	-73

2. test, 437 MHz, CW mode, 2. generator

S-meter (radio display)	S-meter reading (software)	input power – EMF (uV)
0	0	0.2
0	0	0.32
0	0	0.4
0	1	0.6
1	3	0.8
3	6	1.2
4	6	1.6
5	8	2.2
6	9	3.2
8	9	5
9	9+10dB	6.3
9	9+10dB	9
9+5dB	9+10dB	12.6
9+10dB	9+10dB	18
9+10dB	9+20dB	25.1
9+15dB	9+20dB	35
9+20dB	9+20dB	50.2
9+30dB	9+30dB	160

3. test, 437 MHz, CW mode, 2. generator

S-meter (radio display)	S-meter reading (software)	input power – EMF (uV)
0	0	0.02
0	0	0.04
0	0	0.079
0	0	0.16
0	0	0.32
0	0	0.63
0	1	0.71
0	2	0.8
0	3	0.89
1	4	1
2	5	1.1
2	5	1.3
3	6	1.4
3	6	1.6
4	7	1.8
4	7	2
5	7	2.2
5	8	2.5
6	8	2.8
6	8	3.2
7	9	3.6
7	9	4
7	9	4.5
8	9	5
8	9	5.6
8	9	6.3
9	9+10dB	7.1
9+5dB	9+10dB	16
9+10dB	9+20dB	25
9+20dB	9+20dB	50
9+25dB	9+30dB	90
9+30dB	9+30dB	160

4. test, 437 MHz, CW mode, 3. generator

S-meter (radio display)	input power – EMF (uV)
0	0.2
0	0.32
0	0.4
0	0.6
1	0.8
2	1.2
3	1.6
5	2.2
6	3.2
7	5
8	6.3
9	9
9+5dB	12.6
9+5dB	18
9+10dB	25.1
9+15dB	35
9+20dB	50.2
9+30dB	160

5. test, 437 MHz, CW mode, 1. generator

S-meter (radio display)	S-meter reading (software)	input power (dBm)
0	0	-115
0	0	-114
0	1	-113
0	2	-112
0	3	-111
1	4	-110
2	5	-109
3	6	-108
4	6	-107
4	7	-106
5	7	-105
5	8	-104
6	8	-103
6	8	-102
7	9	-101
7	9	-100
8	9	-99
8	9+5dB	-98
8	9+5dB	-97
9	9+5dB	-96
9	9+10dB	-95
9	9+10dB	-94
9	9+10dB	-93
9	9+10dB	-92
9+5dB	9+10dB	-91
9+5dB	9+15dB	-90
9+5dB	9+15dB	-89
9+5dB	9+15dB	-88
9+10dB	9+20dB	-87
9+10dB	9+20dB	-86
9+10dB	9+20dB	-85
9+10dB	9+20dB	-84
9+15dB	9+20dB	-83
9+15dB	9+20dB	-82
9+15dB	9+25dB	-81
9+15dB	9+25dB	-80
9+20dB	9+25dB	-79
9+20dB	9+25dB	-78
9+20dB	9+30dB	-77
9+20dB	9+30dB	-76
9+25dB	9+30dB	-75
9+25dB	9+30dB	-74
9+25dB	9+30dB	-73
9+25dB	9+35dB	-72
9+30dB	9+35dB	-71
9+30dB	9+35dB	-70
9+30dB	9+35dB	-69
9+30dB	9+40dB	-68

7.2 Calibration of the VHF input

1. test, 145 MHz, CW mode, 2. generator

S-meter (radio display)	input power – EMF (uV)
0	0.2
0	0.32
0	0.4
0	0.6
0	0.8
2	1.2
3	1.6
5	2.2
6	3.2
7	5
8	6.3
9	9
9	12.6
9+5dB	18
9+10dB	25.1
9+15dB	35
9+15dB	50.2
9+25dB	100
9+30dB	160

2. test, 145 MHz, CW mode, 1. generator

S-meter (radio display)	S-meter reading (software)	input power – EMF (uV)
0	0	0.63
0	0	0.71
0	1	0.8
0	2	0.89
0	3	1
1	4	1.1
1	5	1.3
2	5	1.4
3	6	1.6
3	6	1.8
4	7	2
4	7	2.2
5	7	2.5
5	8	2.8
6	8	3.2
6	8	3.6
7	9	4
7	9	4.5
7	9	5
8	9	5.6
8	9	6.3
8	9	7.1
9	9+10dB	10
9+5dB	9+10dB	16
9+10dB	9+20dB	25
9+15dB	9+20dB	50
9+20dB	9+30dB	90
9+30dB	9+30dB	160

3. test, 145 MHz, CW mode, 1. generator

S-meter (radio display)	S-meter reading (software)	input power (dBm)
0	0	-115
0	0	-114
0	0	-113
0	1	-112
0	2	-111
0	3	-110
1	4	-109
2	5	-108
2	5	-107
3	6	-106
4	6	-105
4	7	-104
5	7	-103
5	8	-102
6	8	-101
6	8	-100
7	9	-99
7	9	-98
7	9	-97
8	9+5dB	-96
8	9+5dB	-95
8	9+5dB	-94
9	9+10dB	-93
9	9+10dB	-92
9	9+10dB	-91
9	9+10dB	-90
9	9+10dB	-89
9+5dB	9+15dB	-88
9+5dB	9+15dB	-87
9+5dB	9+15dB	-86
9+5dB	9+15dB	-85
9+10dB	9+20dB	-84
9+10dB	9+20dB	-83
9+10dB	9+20dB	-82
9+10dB	9+20dB	-81
9+15dB	9+20dB	-80
9+15dB	9+20dB	-79
9+15dB	9+25dB	-78
9+15dB	9+25dB	-77
9+20dB	9+25dB	-76
9+20dB	9+25dB	-75
9+20dB	9+30dB	-74
9+20dB	9+30dB	-73
9+25dB	9+30dB	-72
9+25dB	9+30dB	-71
9+25dB	9+30dB	-70
9+25dB	9+30dB	-69
9+30dB	9+30dB	-68

Appendix B: Satellite signal strength measurements at UHF band

All the distances and S-meter readings are recorded from the Ham Radio Deluxe software as it was with the default settings.

1. measurement,
Date and time:
13.02.2009, 16:20-16:25
Satellite: XI-IV
Weather: cloudy

Distance (km)	S-meter reading
2400	7
2500	4
2700	6
3100	4

2. measurement
Date and time:
13.02.2009, 17:51-18:07
Satellite: XI-IV
Weather: cloudy

Distance (km)	S-meter reading
2800	5
2500	2
2200	5
1900	5
1600	4
1300	5
1000	2
800	2
1000	8
1300	9
1600	9
1900	9
2200	7
2500	5
2800	7
3100	7

3. measurement
Date and time:
14.02.2009, time 9:27-9:37
Satellite: XI-IV
Weather: cloudy

Distance (km)	S-meter reading
3000	4
2800	rotator problems
2600	5
2500	5
2500	4
2700	8
3000	7
3100	3

4. measurement
Date and time: 14.02.2009, time 9:57-10:10
Satellite:XI-V
Weather: cloudy

Distance (km)	S-meter reading
3000	2
2800	3
2600	3
2400	3
2200	3
2000	2
1800	2
1600	3
1400	3
1200	5
1000	7
800	rotator problems
900	8
1100	6
1400	rotator problems
1600	4
1800	5
2000	7
2200	6
2400	6
2600	6
2800	5
3000	2

5. measurement
Date and time: 14.02.2009, time 10:47-11:00
Satellite: Compass-1
Weather: cloudy

Distance (km)	S-meter reading
3000	rotator problems
2800	rotator problems
2600	4
2400	rotator problems
2200	5
2000	6
1800	6
1600	7
1400	2
1200	2
1000	2
800	2
1000	rotator problems
1200	rotator problems
1400	7
1600	8
1800	8
2000	2
2200	2
2400	2
2600	2
2800	2
3000	2

6. measurement
Date and time: 14.02.2009, time 11:35-11:47
Satellite: XI-V
Weather: cloudy

Distance (km)	S-meter reading
2000	8
2200	8
2400	7
2600	7
2800	6
3000	4

7. measurement
Date and time: 14.02.2009, time 12:23-12:34
Satellite: Compass-1
Weather: cloudy

Distance (km)	S-meter reading
3000	2
2800	2
2600	2
2400	7
2200	8
2000	2
1800	2
2000	9
2200	2
2400	2
2600	2
2800	4
3000	2

8. measurement
Date and time:
15.02.2009, time 9:07-9:19
Satellite: XI-IV
Weather: clear

Distance (km)	**S-meter reading**
3000	rotator problems
2800	rotator problems
2600	7
2400	9
2200	7
2400	9
2600	7
2800	6
3000	8

9. measurement
Date and time:
15.02.2009, time 9:30-9:41
Satellite: XI-V
Weather: clear

Distance (km)	**S-meter reading**
3000	rotator problems
2800	rotator problems
2600	rotator problems
2400	rotator problems
2200	2
2000	2
1800	2
1600	9+5dB
1400	2
1600	2
1800	2
2000	8
2200	6
2400	2
2600	2
2800	2
3000	2

10. measurement
Date and time:
15.02.2009, time 10:36-10:50
Satellite: XI-V
Weather: clear

Distance (km)	**S-meter reading**
3000	6
2800	7
2600	7
2400	8
2200	7
2000	6
1800	8
1600	8
1400	7
1200	5
1000	9
900	9+5dB
1000	9+5dB
1200	9
1400	9
1600	9
1800	9
2000	9
2200	9
2400	8
2600	8
2800	7
3000	7

11. measurement **Date and time:** **15.02.2009, time 11:05-11:18** **Satellite: Compass-1** **Weather: nearly clear**	
Distance (km)	**S-meter reading**
3000	2
2800	2
2600	2
2400	2
2200	9
2000	9
1800	9
1600	rotator problems
1400	rotator problems
1200	rotator problems
1000	9+5dB
800	9+10dB
1000	2
1200	2
1400	6
1600	6
1800	6
2000	2
2200	2
2400	2
2600	2
2800	2
3000	2

12. measurement **Date and time:** **16.02.2009, time 18:33-18:48** **Satellite: XI-IV** **Weather: raining**	
Distance (km)	**S-meter reading**
3000	8
2800	6
2600	5
2400	5
2200	5
2000	6
1800	8
1600	9
1400	8
1200	7
1400	8
1600	9
1800	9
2000	8
2200	7
2400	6
2600	5
2800	5
3000	6

13. measurement **Date and time:** **17.02.2009, time 22:14-22:26** **Satellite: XI-V** **Weather: raining**	
Distance (km)	**S-meter reading**
3000	4
2800	8
2600	8
2400	6
2200	7
2000	6
1800	6
1600	8
1400	8
1600	6
1800	3
2000	4
2200	6
2400	8
2600	8
2800	7
3000	5

14. measurement
Date and time: 17.02.2009, time 22:42-22:54
Satellite: Compass-1
Weather: raining

Distance (km)	S-meter reading
3000	2
2800	2
2600	2
2400	2
2200	9
2000	9
1800	2
1600	2
1400	9
1600	2
1800	2
2000	2
2200	8
2400	8
2600	2
2800	2
3000	2

15. measurement
Date and time: 09.03.2009, time 10:40-10:51
Satellite: XI-V
Weather: cloudy

Distance (km)	S-meter reading
3000	
2800	6
2600	6
2400	6
2200	8
2000	6
1800	4
1600	rotator problems
1400	rotator problems
1200	7
1000	9+10dB
1000	9+10dB
1200	9+10dB
1400	8
1600	8
1800	8
2000	7
2200	7
2400	8
2600	8
2800	8
3000	7

16. measurement
Date and time: 10.03.2009, time 10:12-10:24
Satellite: Compass-1
Weather cloudy

Distance (km)	S-meter reading
3000	3
2800	3
2600	3
2400	9
2200	9
2000	8
1800	2
1600	2
1400	2
1200	2
1000	9
800	9
1000	1
1200	1
1400	1
1600	1
1800	1
2000	1
2200	1
2400	1
2600	1
2800	1
3000	8

8 Appendix C: VHF noise mapping at ISU Ground Station

The values in the tables indicate the S-meter readings of the Ham Radio Deluxe software, where ‘x’ indicates ‘not measured’. The frequency listened was 145.900 MHz and pre-amplifier was switched on.

20.02.2009,		**Elevation (degrees)**				
time 17:00		**8**	**25**	**45**	**70**	**90**
	0	6	2	1	1	0
	30	5	2	0	x	x
	60	4	1	0	x	x
	90	6	4	1	0	x
	120	7	4	1	x	x
	150	5	3	2	x	x
	180	5	2	3	0	x
	210	5	2	2	x	x
	240	5	4	2	x	x
	270	6	5	3	1	x
	300	6	5	4	x	x
	330	6	4	3	x	x

Azimuth (degees)

10.03.2009,		**Elevation (degrees)**				
time 14:00		**8**	**25**	**45**	**70**	**90**
	0	6	4	1	1	0
	30	5	3	1	x	x
	60	5	2	1	x	x
	90	6	5	1	1	x
	120	7	5	1	x	x
	150	5	3	0	x	x
	180	3	1	1	1	x
	210	1	2	1	x	x
	240	3	3	1	x	x
	270	6	3	2	1	x
	300	6	3	2	x	x
	330	6	4	0	x	x

Azimuth (degees)

9 Appendix D: Calibration of the S-meter Capturing software IC-910H Tester

9.1 UHF Calibration Results

The Marconi Instruments 2022 signal generator was connected to the transceivers UHF input and a 437 MHz signal was applied. The signal strength was incremented with 1 dB steps.

Input power (dBm)	'S'-meter reading
-120	5
-119	5
-118	5
-117	5
-116	5
-115	7
-114	16
-113	35
-112	49
-111	58
-110	67
-109	72
-108	78
-107	85
-106	90
-105	96
-104	99
-103	103
-102	106
-101	110
-100	113
-99	117
-98	120
-97	122
-96	126
-95	128
-94	129
-93	130
-92	133
-91	136
-90	138
-89	142
-88	145
-87	146
-86	148
-85	151
-84	154
-83	155
-82	157
-81	160
-80	161
-79	164
-78	165
-77	168
-76	170
-75	173
-74	174
-73	177
-72	179
-71	182
-70	183
-69	186
-68	189
-67	190
-66	193
-65	195

9.2 VHF Calibration Results

The Marconi Instruments 2022 signal generator was connected to the transceivers VHF input and a 145.9 MHz signal was applied. The signal strength was incremented with 1 dB steps.

Input power (dBm)	'S'-meter reading
-120	1
-119	1
-118	1
-117	1
-116	1
-115	1
-114	3
-113	16
-112	33
-111	48
-110	56
-109	65
-108	72
-107	82
-106	85
-105	92
-104	94
-103	97
-102	103
-101	106
-100	110
-99	113
-98	117
-97	119
-96	122
-95	126
-94	128
-93	129
-92	132
-91	133
-90	136
-89	138
-88	141
-87	142
-86	145
-85	148
-84	149
-83	151
-82	154
-81	155
-80	158
-79	160
-78	163
-77	164
-76	165
-75	168
-74	170
-73	173
-72	174
-71	177
-70	179
-69	182
-68	183
-67	186
-66	187
-65	190

10 Satelliitide signaali tugevuste mõõtmine Rahvusvahelise Kosmoseülikooli ja Tartu Ülikooli tugijaamaga

10.1 Kokkuvõte

Käesoleva töö eesmärgiks oli satelliitide signaalide kvantitatiivne mõõtmine Rahvusvahelise Kosmoseülikooli tugijaamaga ning satelliidi signaalide ja tugijaama tehnika parem tundma õppimine töö käigus. Töö hõlmas meetodite ja tarkvara arendamist, mida saab kasutada edasisteks uurimusteks nii Rahvusvahelises Kosmoseülikoolis kui ka Tartu Ülikoolis. Töö käigus omandatud kogemused on väga väärtuslikud mitte ainult Tartu Ülikooli satelliitside tugijaama edasisel arendamisel vaid ka Eesti Tudengisatelliidi projektile tervikuna ning teistele võimalikele tuleviku projektidele.

Tähtsamad tulemused:

- Icom IC-910H transsiiveri kalibreerimise tulemused olid kooskõlas varem avaldatutega (Flechtner, 2001). Maksimaalsed erinevused olid ainult 3 dB, järelikult signaali generaatori puudumisel võib nimetatud allika tulemusi etalonina kasutada.
- Prof. Joachim Köppeni kirjutatud transiiveri S-meetri salvestustarkvara IC910Tester osutus väga kasulikuks ja töökindlaks. IC910Testerit võib kasutada ka tulevikus satelliitide signaali tugevuste salvestamiseks.
- UHF sagedusalas tehtud mõõtmised olid arvutustega kooskõlas. Salvestatud signaalide maksimumväärtused olid reeglina arvutustega samad või mitte rohkem kui 3 dB nõrgemad.
- Tugeva müra tõttu 145.900 MHz sagedusel VHF laineala mõõtmised ebaõnnestusid. Müra kaardistamisel selgus, et müra on tugevam just nendel suundadel, kus tugijaama lähedal on veel teisi ehitisi.

- Kuupsat Cute-1 majaka signaal osutus spetsifikatsioonis märgitud 100mW 3-5 dB tugevamaks. Mõõtmisviga on vähetõenäoline, sest kõikide teiste mõõdetud kuupsatelliitide (Compass-1, XI-IV, XI-V) signaalid andsid arvutustega kooskõlas tulemusi.
- Mõnedel satelliidi ülelendudel avaldus huvitav efekt – horisondi lähedal (2º-6º tõusunurgaga) oli signaal eeldatust kuni 7 dB tugevam. Võimalik põhjendus on seotud UHF lainete levikuga atmosfääris, kuid võimenduse tekkimise mehhanism on veel üsna ebaselge.
- Enamikul ülelendudel oli satelliidi tugijaamale lähenedes signaal märgatavalt nõrgem (kuni 10 dB), kui satelliidi eemalduval harul. Lähem uurimine näitas, et efekt esines eelistatult teatud suundadel – asimuutidel 40º-100º ja 300º-340º ning tõusunurgaga vähemalt 17º.
- Cute-1 ja XI-IV signaalide tugev (5-10 dB) perioodiline varieerumine vihjab, et nad laperdavad kosmoses juhuslikult. On teada, et Cute-1 ei ole orientatsioonikontrolli (Kawakubo, 2009) ning XI-IV on (Komatsu, 2009). Signaalide väga sarnane käitumine vihjab, et XI-IV orientatsioonikontroll ei ole töökorras.
- Tartu Ülikooli tugijaamaga salvestatud satelliidi ülelennu audiofaili analüüs näitas, et isegi sellise kaudse meetodiga on võimalik signaali üldist käitumist hinnata.